Questa Baseline and Pre-mining Ground-water Quality Investigation 8. Lake-sediment geochemical record from 1960 to 2002, Eagle Rock and Fawn Lakes, Taos County, New Mexico

By S.E. Church, D.L. Fey, and M.E. Marot

Abstract

Geochemical studies of lake sediment from Eagle Rock Lake and Fawn Lake were conducted to evaluate the effect of mining at the Molycorp Questa porphyry Mo deposit located immediately north of the Red River. Two cores were taken, one from each lake near the outlet where the sediment was thinnest, and they were sampled at 1-cm intervals to provide geochemical data at less than 1-year resolution. Samples from the core intervals were digested and analyzed for 34 elements using ICP-AES. The activity of ^{137}Cs has been used to establish the beginning of sedimentation in the two lakes. Correlation of the geochemistry of heavy-mineral suites in the cores from both Fawn and Eagle Rock Lakes has been used to develop a sedimentation model to date the intervals sampled. The core from Fawn Lake, located upstream of the deposit, provided a continuous sedimentary record of the geochemical baseline for material being transported in the Red River whereas the core from Eagle Rock Lake, located downstream of the deposit, provided a continuous record of the effect of mining at Questa on the sediment in the Red River. Abrupt changes in the concentrations of many lithophile and deposit-related metals occur in the middle of the Eagle Rock Lake core, which we correlate with the major flood of record recorded at the Questa gage at Eagle Rock Lake in 1979. Loss of mill tailings via documented pipeline breaks are shown to be responsible for some of the spikes in trace-element concentrations in the Eagle Rock Lake core. Sediment from the Red River collected *at low flow* in 2002 is a poor match for the geochemical data from the sediment core in Eagle Rock Lake. The change in sediment geochemistry in Eagle Rock Lake in the post-1979 interval is profound and requires that a new source of sediment be identified that has substantially different geochemistry from that in the pre-1979 core interval. We hypothesize that this source was introduced onto the floodplain of the Red River during the 1979 flood-of-record and has been redistributed by channelization of the Red River following the flood. Comparisons of the geochemistry of the post-1979 sediment core with both mine wastes and with premining sediment from the vicinity of the Questa mine indicate that both are possible sources for this new component of sediment. Existing data have not resolved this enigma.

Introduction

The Molycorp Questa molybdenum mine, located in the Taos Range in north central New Mexico, is currently producing molybdenum concentrate and is in the process of developing a mine-closure plan. This report is one of a series of reports designed to determine geochemical baselines and the pre-mining ground-water quality for the Red River valley at the site. The Red River, which follows the southern bounding fault of the Questa caldera, flows past the Questa porphyry molybdenum deposit. Fawn Lake, located on the Red River upstream of the Questa deposit (fig. 1), is small, covering an area of about 1 hectare, and provides a continuous sedimentary record for the period from 1960 to the present. Eagle Rock Lake, located downstream of the Questa deposit (fig. 1), covers about 2 hectares and provides a continuous sedimentary record of material transported away from the Questa mine site as well for sites upstream. A comparison between the sedimentary records provides a measure of the impact of development of the Questa mine, which began as an open-pit operation in 1965. Although there was base-metal mining upstream in the early 1900's, the previous mining activity appears as a part of the geochemical baseline recorded in Fawn Lakes. Our study focuses on the determination of the geochemical signature in sediment transported by the Red River prior to mining as well as that transported today, and the effect of recent mining activity on the sedimentary record in a core from Eagle Rock Lake. Fawn Lake was sampled as a background site to document the temporal variation of metals supplied by erosion in the Red River valley. Both ponds originated as borrow pits during road construction and paving of NM Highway 38 in 1960-1961 (Miguel Gabalgon, New Mexico Highway Dept., personal commun, Sept. 2003). A portion of the water from Red River flows through both Fawn Lakes and Eagle Rock Lake. Flow is regulated to about 2 cfs by head gates installed by the irrigation company that owns the surface water rights. The head gates serve as baffles that limit flow and thus limit the amount of sediment deposited in the lakes during high flow.

Geologic Setting

The Questa porphyry molybdenum mine lies along the southern margin of the Questa caldera, which is part of the late Oligocene Latir volcanic field in north-central New Mexico (Lipman, 1981). The Latir volcanic field consists primarily of mildly alkaline intermediate-composition lavas 1- to 2-km in thickness that overlie Proterozoic crystalline basement consisting of metasedimentary and metavolcanic rocks that are intruded by numerous granitic plutons (Lipman and Reed, 1989; Ross and others, 2002). Andesite and quartz latite flows predate caldera formation. Volcanism culminated in the eruption of the peralkaline Amalia Tuff (Lipman and others, 1986; Johnson and Lipman, 1988) and formation of the

Questa caldera at about 25.7 Ma (Czamanske and others, 1990; Ross and others, 2002). Ludington and others (2003) provide the geologic framework of the Red River watershed pertinent to this study.

The Tertiary volcanic rocks were subsequently intruded by a series of highly evolved, high-silica granites and subvolcanic porphyries (Johnson and others, 1989; Ross and others, 2002) that are the apparent sources of the hydrothermal fluids that formed the molybdenite deposits. The Bear Canyon and Sulfur Gulch stocks are associated with the molybdenum mineralization and are characterized by high concentrations of Y, Zr, and the rare earth elements (REE), and low concentrations of Ba and Sr (Johnson and others, 1989; Ludington and others, 2004). These granites and porphyries were emplaced after 24.6 ± 0.1 Ma, and appear along a N75E trend that extends from the Bear Canyon stock at the western range front into the Red River intrusive complex northeast of the town of Red River. Mineralization in the Questa system is dated at 24.1 ± 0.2 Ma (Ross and others, 2002 and fig. 2) and is comparable with other Climax-type, high-silica granitic stockwork molybdenite deposits (Carten and others, 1993). An elongate granitic batholith is inferred at depth, which served as the parent body to the high-level stocks that gave rise to the known mineral deposits. The Questa deposit contains molybdenum mineralization in quartz stockwork with minor galena, sphalerite, and chalcopyrite along with fluorite and carbonate minerals (Carpenter, 1968; Ross and others, 2002). Two ore bodies have been mined underground, the Goat Hill (1983 - 2000) and D ore bodies (2001 - present). Both have molybdenite-bearing ore zones followed by late-stage magmatic hydrothermal breccia (Ross and others, 2002) that contain abundant quartz-carbonate-fluorite veins. Ross and others (2002) estimate that the volume of the hydrothermal breccia in the Goat Hill ore body was 10-15 percent. Several generations of brecciation have been identified; fluorite occurs in the latest generation of hydrothermal breccias (primarily in zones D and E, table 3 and fig. 7, Ross and others, 2002).

Hydrothermal alteration related to mineralization processes can be found along the entire length of the mineralized trend. The upper part of the Questa deposit has been oxidized and the hydrothermal alteration assemblages are exposed at the surface. The alteration assemblages, as mapped by AVIRIS (Livo and Clark, 2002), appear to be dependent upon the nature of the underlying mineralization and the amount of host rock cover over the mineralized porphyries. Alteration associated directly with the molybdenite mineralization is potassic, and includes assemblages containing hydrothermal biotite and orthoclase (Carpenter, 1968, Ross and others, 2002). Overlying the potassic alteration and the known mineralized rocks, phyllic or quartz-sericite-pyrite (QSP) alteration is present. Within the open pit at Questa, this mineral assemblage is characterized by the presence of sericite, kaolinite, goethite, and jarosite (Livo and Clark, 2002). At Questa, as at other Climax-type molybdenite systems, QSP alteration is peripheral to the underlying molybdenite-bearing rock. Distal to QSP alteration, both laterally and vertically, widespread propylitic alteration (epidote, chlorite, and calcite) is encountered. It is characterized here in the AVIRIS image by combinations of epidote and epidote plus calcite (Livo and Clark, 2002).

Meyer and Leonardson (1990) identified additional areas of hydrothermal alteration exposed upstream from the Questa deposit (fig. 1). These areas have also been mapped by AVIRIS (Livo and Clark, 2002) and are discussed in detail by Ludington and others (2003). These altered scarred areas are subject to rapid erosion of hydrothermally altered rock along the N75E trend above the inferred batholith. These steep barren drainages are formed by mass wasting and rapid erosion of the highly altered rock and are the result of landslides, slumps, rock falls, and fluvial processes. In the AVIRIS images, the erosional scars are surrounded by propylitic mineral assemblages, but within the scars, QSP alteration assemblages contain kaolinite, sericite, jarosite and goethite (Livo and Clark, 2002). Although supergene alteration minerals like kaolinite and gypsum are commonly observed, exposures of bedrock usually exhibit primary alteration assemblages, most commonly QSP. A large proportion of the erosion that occurs in these altered areas takes place during intense precipitation periods due to summer thunderstorms, as well as during the spring snowmelt. At these times, large amounts of sediment-laden water runs off the base of the scars and has formed large debris aprons at their base. These debris aprons consist of poorly sorted material, rich in pyrite and other weathering products, that range in size from large blocks with dimensions of tens of meters, down to silt- and clay-sized material. The aprons generally reach the banks of the Red River, and much of this altered material enters the river during periods of high runoff. Large-scale mass wasting from these alteration scars has been suggested as a source of metals in sediment in the Red River. These alteration scars and their geochemistry are discussed in detail in Ludington and others (2003). Three of these altered scar areas, the Hottentot and Straight Creek drainages on the north and June Bug on the south, are upstream of Fawn Lakes (fig. 1). Thus, the sediment contributed by these altered areas is included in the background core from upper Fawn Lake.

Figure 1 near here

History of Mining at Questa

According to Carpenter (1968), mining began in the district in the early 1900's. The town of Red River was established to serve the needs of early gold miners. Various base- and precious-metal deposits hosted in Precambrian rocks were exploited by these early mining ventures (Jackson and others, in press). By 1920, Red River had become a ghost town. Molybdenum Corporation of America acquired the claims at Questa in 1921, and from 1923 to 1958 produced about 20 million lbs of molybdenum using selective underground stope mining methods to recover high-grade molybdenite ore from veins in the main Questa ore body (Ross and others, 2002, table 1).

Open-pit mining began at Questa in 1965 (table 1, Ross and others; 2002). From 1965 - 1981, an estimated 81 Mt of ore was removed. Initial production was 10,000 tons/day (Carpenter, 1968); mill capacity was 15,000 tons/day. A total of 350 Mt of low-grade overburden were removed from the open pit (Dave Jacobs, Unocal, personal commun., 2003). In the open pit, hornblende andesite has undergone potassic alteration (quartz, orthoclase, biotite, sphene, chlorite, epidote, pyrite, and iron oxide minerals). The andesite and overlying andesitic tuff have been completely altered to sericite, chlorite, and carbonate minerals. AVIRIS data (Livo and Clark, 2002) suggest that advanced argillic alteration, as indicated by abundant kaolinite, may be present in the upper alteration zone exposed in the open pit.

From 1983 through 1991 and from late 1996 to 2000, the Goat Hill ore body was mined underground using block-caving methods (fig. 3; Ross and others, 2002; Dave Jacobs, personal commun., 2003). During this period, 21 Mt of ore were removed and processed at the Questa mill. The Goat Hill ore body was intruded into the overlying andesitic flows, and is a breccia body in a late-phase granitic intrusive. The Goat Hill ore body contains a higher grade of MoS_2 than the open-pit ore body (Ross and others, 2002). Ross and others (2002) indicate that the Goat Hill ore body consists primarily of quartz, molybdenite, pyrite, calcite, fluorite, anhydrite, and gypsum in an aplite matrix that intruded the overlying andesite flows. Hydrothermal biotite (phlogophite), orthoclase, calcite, fluorite and quartz are listed as alteration or gangue minerals (table 3 and fig. 7, Ross and others, 2002). Potassic alteration is extensive in the ore zone of the Goat Hill ore body (Leonardson and others, 1983).

In 2001, Molycorp began mining the D ore body again using block-caving methods. This ore body is very similar to the Goat Hill ore body and has similar chemistry and mineralogy (Leonardson and others, 1983; Ross and others, 2002).

Previous Geochemical Studies

The general area on either side of the Questa deposit was studied and mapped during the USGS Wilderness program in the early 1980's. The Red River generally follows the southern margin of the Questa caldera. Volcanic rocks of the caldera are in fault contact with Precambrian rocks, which are exposed on the south side of Red River. Tributary streams draining north from this Precambrian terrane, with the exception of Columbine Creek, are in Precambrian rocks and have no geochemical anomalies in stream sediment (Sutley and others, 1982). The Questa deposit lies in the caldera on the north side of the Red River (fig. 1). Stream-sediment samples taken from tributaries draining the north side of Cabresto Creek, the drainage to the north of the Questa block, also had no geochemical anomalies indicative of a Climax-type porphyry molybdenum deposit. No data were collected from the area between Red River and Cabresto Creek during the USGS Wilderness assessment studies.

In 1976, the National Uranium Resource Evaluation Project (NURE) sampled sediment in surface streams in the vicinity of the Questa mine. Sediment was sampled in tributaries on both sides of the Red River and analyzed by Inductively Coupled Plasma Atomic Emission Spectroscopy (ICP-AES) at Oak Ridge National Laboratory (NURE, 1981). These data provide a 1976 geochemical baseline during the period when the open pit was in operation (fig. 1).

Allen and others (1999) conducted a study of the sediment geochemistry in the Red River and in the two lakes discussed here. They sampled cores from each of the two lakes and from seven localities along the Red River between the towns of Red River and Questa. Lake cores were taken near the inlet and outlet of the lakes. Samples were collected and dried. Following digestion, they were analyzed for Al, Fe, Mn, Co, Cu, Mo, Ni and Zn by atomic absorption. There was no age control on these cores. Concentration data were reported from 11 intervals from Eagle Rock Lake core C1 (1.6 m depth), for 12 intervals from Eagle Rock Lake core C2 (0.7 m depth), and from 11 intervals from the Fawn Lake core (1.4 m depth).

Jackson and others (in press) have recently completed a stream-sediment study of the Red River watershed upstream of Red River.

Methods

Sampling Plan

We used a pontoon boat to sample lake sediment from Fawn and Eagle Rock Lakes on consecutive days in summer, 2002 (fig. 2). We anchored the boat in the deepest part of each lake, away from the inlet, in an attempt to minimize the effects of storm deposits on the thickness of individual strata in the cores. We sampled the lake sediment by driving a 7.6-cm diameter polycarbonate coring tube into the sediment and then extracting it using a hoist. The cores were driven to resistate; coarse angular monolithic rock fragments were recovered in the basal 1-cm section from each core. We recovered the entire lake-sediment stratigraphy from both lakes (a 50-cm core from Fawn Lake and 55-cm core from Eagle Rock Lake). No discernable stratigraphy was visible in the lake cores and all material was silt and clay-sized. The core samples were sectioned at 1-cm intervals, placed in plastic bags, sealed, and shipped to the laboratory for processing. To evaluate the source of sediment in the lake cores, we sampled modern stream sediment from the active alluvium of Red River and pre-mining sediment from preserved terraces along the course of the river to determine the modern and pre-mining geochemical baseline. Sampling methods for the pre-mining baseline sampling have been previously described in Church and others (2000). We also sampled sediment from six creeks draining the alteration scars upstream of the Questa mine (fig. 1) to determine the type of sediment material being supplied by the scar areas to the

Red River and we collected composite samples of ten terrace fans in the study area to evaluate spatial variability.

At the laboratory, the lake-sediment samples were air dried and split prior to analysis. Fan and stream-sediment samples were sieved to minus 80 mesh and ground prior to chemical analysis.

Figure 2 near here

Analytical Methods

The lake-sediment samples were analyzed for loss on ignition (LOI) to remove organic material by heating in a muffle furnace at 450° C for 6 hours. Selected samples were counted using a Canberra intrinsic germanium detector to determine the depth of the maximum ^{137}Cs activity. This peak activity was assigned a date of 1963 which corresponds to the maximum fallout activity from atmospheric nuclear testing. Analytical results are in the appendix, tables A1 and A2. In both cases, the ^{137}Cs peak occurred a few cm above the bottom of the core, which is confirmation that the estimated date of construction of the ponds was 1961. Thus, the Eagle Rock Lake core contains the entire record of sedimentation over the period of operation of the Questa mine beginning with the development of the open pit mine in 1965 and has a resolution of about 1 year (50-55 sampling intervals over a 41 year period).

Stream-sediment, lake-sediment, mill tailings, and the terrace composite samples collected for this study were analyzed using ICP-AES methods following a mixed acid total digestion (HCl, HNO_3, HF, and $HClO_4$; Briggs, 1996). QAQC results have been documented in Fey and others (1999). Analytical results are in the appendix, table A3.

Samples of the megabreccia from the D ore body were supplied by Megan Jackson (Molycorp, 2003) for analysis. Three of the samples were disaggregated and separated into discrete phases, a light green phase (fluorite) and a white phase (carbonate), for analysis. The samples were digested in hot HNO_3 and the soluble phase dissolved for analysis. The residues were digested using the mixed acid total digestion (HCl, HNO_3, HF, and $HClO_4$; Briggs, 1996), although additional $HClO_4$ was added to insure that insoluble REE fluoride minerals did not form. These data are given in the text below.

Stream Flow Recorded at the Questa Gage

Stream-flow measurements of surface-water discharge have been recorded at the gage at Questa, New Mexico (08265000) for 74 years. The stream gage is immediately upstream from Eagle Rock Lake (fig. 1). Data show that the flood of record occurred in 1979 (fig. 3). Runoff exceeded 300 cfs for 44 days and had an average peak daily flow of 557 cfs on June 9, 1979. Stream-flow data (1960 to Sept. 30, 2002), where greater than 300 cfs, are in table 1 (http://nm.waterdata.usgs.gov/nwis). Periods of peak stream flow correlate well with changes in geochemistry of the core from Eagle Rock Lake.

Table 1 and Figure 3 near here

Discussion

Lake Sediment Chronology

The ^{137}Cs data from both lakes showed a pronounced peak in activity at depths of 2 and 4 cm above the base of the core (fig. 4). Given that the lakes are in two borrow pits that were constructed in 1960-1961 for the purpose of road construction, this setting is ideal for application of the ^{137}Cs dating method. The ages were calculated assuming that the depth at maximum ^{137}Cs activity occurred at the peak of atmospheric nuclear testing activity in 1963. We used the geochemical data for those elements not associated with the molybdenum mine at Questa to adjust the lower portion of the ^{137}Cs curve from Eagle Rock Lake to match that from Fawn Lake. Stream-flow data indicate that the flood of record occurred in 1979 (table 1). Hydrologic data indicate that the period prior to the flood was somewhat drier than the period after the flood. Numerous changes in the concentrations of both major and minor elements occurred at about the middle of each core, which we have associated with this period. We have assumed many of these changes in core sediment geochemistry are related to the 1979 flood and have created a sedimentation model to fit these age constraints that reflect these slightly different sedimentation rates (fig. 5). Comparison of the hydrograph constructed using the monthly average flow over the period of 1960-2002 does not result in a perfect match between peak flow values and large increases in metal concentrations (see figures and the discussion in the following section), but many of those peak metal concentrations were close to peak flows. We have no independent data to warrant further adjustments in the sedimentation rate in the two lakes or to suggest that the sedimentation rates in the two lakes differed significantly one from another. We decided that any further adjustments would be ad hoc and were not justifiable. The resulting model gives a good correlation of peaks in metal concentrations between lakes and highlights the difference between the sediment in both cores with better than 1-year resolution. Spikes in metal concentrations in both lakes can be associated with smaller flood events recorded at the Questa gage (table 1).

Figures 4 and 5 near here

Lake Sediment Geochemistry

Sedimentation in the two lakes is remarkably constant as shown by the sedimentation model (fig. 5). The presence of the head gates that limit the inflow to the lakes to approximately 2 cfs has resulted in reducing the amount of sediment transported into the lakes at high flow. The distribution of major and trace elements in sediment cored from Eagle Rock Lake and Fawn Lake is in figures 6 – 10, plotted as a function of calculated age on the basis of the sedimentation model (fig. 5). Peak spikes in concentration of the major and trace elements are summarized in the chart in table 2. Peaks were defined as elevated concentrations of individual elements that generally occur over a short period of time relative to the time frame of the record in the core. Sharp peaks were recorded only over the period where the half-width exceeded the half-height of the peak. We have grouped the elements in terms of their primary mineralogical residence sites in silicic rocks such as occur in the study area.

Table 2 near here

Element Patterns

The sedimentary record cored in Fawn Lake differs markedly from that cored in Eagle Rock Lake (table 2, figs. 6 – 9). For the most part, the geochemical data from sediment from Fawn Lake show minor variations throughout the period sampled. The single most striking feature of the geochemical data from the Fawn Lake core is the large number of trace elements that were concentrated during what we interpret as the 1979 flood event. Many of the trace elements enriched at this depth in the core occur primarily or exclusively in heavy-mineral phases that would be mobilized during high flow (table 2). Minerals identified by x-ray defraction in the Fawn Lake core sample (02QNM102LY at the 1979 peak) include quartz with minor amounts of montmorillonite, muscovite (illite or sericite), kaolinite, and a potassium feldspar (R. Driscoll, written commun., 2003). In contrast, data from sediments from Eagle Rock Lake are substantially different. Plots of three groups of elements, the Large-Ion-Lithophile (LIL) elements (figs. 9 and 10), the major and minor elements (figs. 6 and 7), and the deposit-related metals (fig. 8) generally show markedly different geochemical behavior in the sediment from Eagle Rock Lake before and after the flood-of-record in 1979 (table 2). Many elements show marked changes in the baseline geochemical concentrations after the 1979 flood. Many of the elements in the heavy-mineral phases (Mo, Cu, Zn, Cd, Ba, Be, and the REE) had peak concentrations during the 1979 flood event. Minerals identified by x-ray defraction in two samples from Eagle Rock Lake. Sample 02QNM101LAX contains quartz, muscovite (illite or sericite), and minor clinochlore. This sample occurs below the depth of the

1979 flood record. Sample 02QMN101LZ (the 1979 peak which contains the highest concentration of Ce) contained quartz and minor amounts of montmorillonite like that found in Fawn Lake. Fluorite and REE-bearing minerals were not found at concentrations sufficient to identify by X-ray diffraction (about 1 percent by volume). No pyrite or molybdenite was identified and no iron oxide minerals that might be carriers of the REE, Nb, and Y were identified (R. Driscoll, written commun., 2003). Correlation of the peak concentrations of the elements associated with heavy-mineral phases and the abrupt change in geochemical baselines at this time (figs. 6-10) is the basis of the calibration of the geochronology of the two cores in 1979 (fig. 5).

Figures 6-10 near here

Element Peaks

Fawn Lake is characterized by occasional peaks in element concentrations above the general geochemical baseline recorded in the sediment core (table 2). The element suite K, Ti, V, Cr, Pb peaks in 1963-66, 1975-78, 1982-83, and 1993-94, and the suite Fe, Si, Ni, Co, Cu, Zn peaks in 1988-1990, which were low-flow years. The element suites Na, Cr, Cu, Zn peak in 1967-72, and Fe, V, Cr, Pb peak in 1993-94, which were high-flow years. The two primary sources for sediment for Fawn Lake are the Precambrian rocks upstream of Red River (Jackson and others, in press), and the alteration scars that occur between Red River and Fawn Lake (fig. 1). Ludington and others document the high erosion rates that occur in the alteration scars during summer rainstorms. The element suites formed during wet years (Fe, V, Cr, Pb) contain many of the elements enriched in sediment from the scar areas (table A3). Finally, there is a pronounced Ca, Al, Si, Sr peak in the core from about 1986-1990 which we interpret as an anthropogenic source, probably concrete associated with building activity in the floodplain in the town of Red River or vicinity.

Peak concentrations in the Eagle Rock Lake core are much more varied and frequent. We identify several different processes that have resulted in the introduction of different trace-element suites into the Red River downstream of Fawn Lake that explain the geochemical record found in the Eagle Rock Lake core. Examination of the elemental associations prior to the 1979 flood shows that the element suite Mg, Fe, Al, Ti, V, Pb peaked during the dry period 1963 – 67, and that the element suite K, Mg, Ti, V, Cr, Pb, Sr, P peaked during wet periods from 1970 – 71 and 1976 – 77 (figs. 6-10 and table 2). However, at the 1979 flood event, the element suite Na, Mg, Ti, V, Cr, Sr shows a marked decrease and the suite Al, Be, Ba, Zn, Cd, Co, Ni, Cu a marked increase (figs. 6-10 and table 2). These fundamental changes indicate a new source of sediment was introduced into the Red River floodplain downstream from Fawn Lakes during the 1979 flood event. We interpret these changes to be the result of a major erosional event that occurred during the flood of 1979.

Comparison of the Data from the Two Lake Sediment Cores

Comparisons of the sediment geochemical data from the two lake cores are in figure 11. Five major elements, Na_2O, MgO, FeO, Al_2O_3, and TiO_2, and six trace elements, Ba, Sr, Cr, V, Cu, and Zn, are presented as box plots to show the difference between sediment deposited in the two lakes before and after 1979. The range of values between the 25^{th} and 75^{th} percentiles is remarkably small for many elements. Figures 11A and B compare element concentrations in sediment from Fawn Lake prior to and subsequent to the 1979 flood. The small ranges and median concentrations from pre-1979 and post-1979 sediment are very similar. In contrast, the geochemical data from Eagle Rock Lake (figs. 11C and D) show the marked contrast between sediment deposited prior and subsequent to the 1979 flood with only Sr, V, and Cr showing little change with time. All five of the major elements showed substantial changes in concentration indicating a new source of sediment following the 1979 flood. In fact, the concentration ranges of the major elements Na_2O, MgO, FeO, Al_2O_3 and TiO_2 do not even overlap between the 25^{th} and 75^{th} percentiles! In figures 11 E and F, we compare the geochemical data from sediment in Eagle Rock Lake from pre-1979 with all of the data from the sediment core from Fawn Lake. Only concentrations of Cu and Zn are elevated in the pre-1979 sediment from Eagle Rock Lake relative to that in sediment from Fawn Lake.

Figure 11 near here

Element Suites that May Be Related to Mining

Different element suites can be associated directly with the mining and processing of ore at the Molycorp Questa mine (table 3). There is a pattern of molybdenum enrichment in the Eagle Rock Lake core from the early 1960's through 1967 (fig. 8). There are also increases in concentrations of Cu, Zn, Co, and Ni (table 3, fig. 8), all of which are either ore metals or halo elements associated with porphyry molybdenum deposits (for example, Carten and others, 1993). We interpret this progressive enrichment with time of this suite of elements to indicate that the beginning of development of the open pit mine at Questa, which began in 1965, was having an increasing effect on the availability of this suite of elements to erosion and transport by the Red River. Concentrations of elements present in the Precambrian rocks in the pyroxene/amphibole suite were reduced with time and concentrations of elements associated with sulfide mineral phases associated with the Questa ore body increased. The most direct and compelling evidence of this hypothesis is the increase of the size of the molybdenum peak with the continued development of the open pit (fig. 8). The Mo peak begins to increase prior to the development of the open pit because the mine waste from the underground vein mining that occurred from 1921-1958 at the site would have had to be removed prior to open pit development.

A second peak of Mo enrichment, which occurs between 1969 – 1975, does not have any other deposit-related metals associated with this buildup (table 3 and fig. 8). We interpret this peak as either a product spill (truck accident) or perhaps a buildup of Mo in the lake sediment following a period of high ore production at the Questa mine. The peak concentration of Mo tailed off quickly suggesting that the peak may have been the result of changes in mill operation that reduced the air pollution from the mill. A similar high peak concentration of Mo deep in the cores from Eagle Rock Lake was also reported by Allen and others (1999). The cause of this peak cannot be determined without access to detailed production and maintenance records from the Questa mill.

There are various peaks in concentration of Cu, Zn, Co, Ni, and REE that are readily explained by breaks in the pipeline that carried mill wastes to the repository. The mill-waste pipeline parallels NM Highway 68 from the mill site (fig. 1) to a tailings repository west of the town of Questa. URS (unpub. report, written commun., 2003) has documented hundreds of pipeline breaks from Molycorp records over the life of the Questa mine. The vast majority of these spills were small and readily cleaned up by Molycorp (URS, written commun., 2003), however, the amount of mill waste reportedly lost to the Red River via pipeline breaks appears to be underestimated. The USDA Forest Service provided us with photographs of the 1981 pipeline break at the Goat Hill Campground (fig. 12). The photographs appear to indicate that a substantial amount of mill waste was lost during this event. Analysis of four mill-waste samples collected in 2003 (table A3) from along the Red River at the Goat Hill, Capulin, and 1979 flood pipeline break sites have remarkably similar compositions and relatively low average metal concentrations (Mo, 340 ppm; Cu, 94 ppm; Pb, 120 ppm; Zn, 170 ppm; Co, 16 ppm; and Ni, 30 ppm). However, a fifth sample of mill waste (03QNM101T) collected inside a piece of pipe in the Molycorp pipeline yard where it had been protected from weathering gave high concentrations of the metals listed in table 3 (Mo, 1,600 ppm; Cu, 1,200 ppm; Pb, 1,600 ppm; Zn, 850 ppm; Co, 820 ppm; and Ni, 630 ppm). Concentrations of As (80 ppm) and Cd (14 ppm) were also elevated in this sample of mill waste (table A3). This suite of metals reside in the sulfide phases in the Questa ore body (Ross and others, 2002) and, with the exception of Mo, they are not recovered in the milling process. Since they occur in sulfide phases, they weather readily and have been leached from the mill tailings exposed on the riverbank subsequent to the pipeline breaks. Concentrations of the REE in this mill tailings sample do not approach peak concentrations of REE found in the core from Eagle Rock Lake (fig. 10 and table A3).

Figure 12 near here

REE Patterns in Fluorite from the Megabreccia in the Questa Ore Body

Concentrations of the REE in the rocks of the Questa caldera are high and enriched in the light REE typical of highly evolved silicic volcanic rocks. Plots of the chondrite-normalized REE data from volcanic and plutonic rocks from the study area (fig. 13 A and B) show that the median REE concentrations from the Fawn Lake core are quite similar to that from the Amalia Tuff and some of the granitic plutons. The range of REE concentrations in sediment from Fawn Lake is small when compared to the range from Eagle Rock Lake. REE concentrations in sediment from the core from Eagle Rock Lake are substantially higher than rocks typical of the evolved rhyolitic Amalia Tuff (fig. 13A), have a small Eu anomaly, and are more enriched than in the peralkaline granite (fig. 13B). Whereas Lipman (1983) and Johnson and others (1989) report lavas that are somewhat more evolved and have greater REE enrichment than those patterns shown in figure 13A, ranges of REE concentrations in the Eagle Rock Lake core far exceed values reported for typical volcanic and plutonic rocks (fig. 13B) from the caldera. Neither the Oligocene volcanic rocks of the Latir caldera nor the REE present in the mill tailings can account for the REE anomalies in the Eagle Rock Lake sediment (fig. 10).

Figure 13 near here

The megabreccia associated with the ore body described in Ross and others (2002) contains abundant fluorite. Since this is the residual or pegmatitic phase from the hydrothermal crystallization process, we requested samples of the megabreccia from Molycorp for chemical analysis to evaluate possible enrichment of the REE in this late crystallization phase of the deposit. Megan Jackson (Molycorp) provided about a dozen samples of the megabreccia from the D ore body and one sample of fluorite from veins exposed in Sulfur Gulch (QSFG, table 4). We analyzed the Sulfur Gulch fluorite and four samples of the megabreccia from the D ore body (fig. 14). Samples were selected on the basis of the variation in texture. Three of the five samples (QF-2, QF-3, and QF-4) were disaggregated and the white and green non-sulfide phases were separated by hand picking for analysis on samples. Sample descriptions accompany figure 14 and the analytical results are in table 4. The white phase was a carbonate-rich phase that was almost completely dissolved in HNO_3. The data from the carbonate phases indicate that they are enriched in Mn and Li, but were not particularly enriched in any of the other trace elements. In contrast, the fluorite phase in samples QF-3 and QF-4, which appeared to be equigranular with discrete banded layers of fluorite and calcite, contained elevated REE concentrations. However, the concentrations are not sufficient to explain the REE anomalies in the Eagle Rock Lake sediment core without some enrichment mechanism. This is in contrast with the data from a more coarsely crystalline vein fluorite and carbonate sample (QF-2) where both Mn and the REE concentrations are not as enriched in either the calcite or fluorite phases in the other two samples. This more coarsely crystalline vein material does have substantially more Ba in the calcite, however, than the other calcite megabreccia samples (table 4). Fluorite from the vein sampled in Sulfur Gulch (QSGF-1) contains low concentrations of Mn, Ba, and the REE. These two samples may represent precursor fluorite veins that formed prior to ore deposition.

Figure 14 and table 4 near here

Electron backscatter photomicrographs taken on the SEM by Sharon Diehl (written commun., 2003) show that three REE-bearing phases occur as small inclusions in the fluorite: a hexagonal mineral identified as synchysite, a Ca, REE-rich carbonate, a REE-rich $CaSO_4$, and a REE-rich Ca phosphate mineral (fig. 15). Geoff Plumlee (oral commun., 2003) initially identified microscopic occurrences of a rare-earth carbonate-fluoride mineral, possibly synchysite, in bedrock drill cuttings from drill hole SC-5B in Straight Creek (Ludington and others, 2004) where the synchysite appears to be associated with hydrothermal quartz-pyrite-carbonate veins and disseminations in the altered rock. The megabreccia forms a substantial component of the ore bodies mined at Questa (B. Walker, Molycorp., oral commun., 2003). Analyses of F in both the sediment from the alteration scars (table A3) and from the Eagle Rock Lake core over the interval where the REE anomaly occurs (table A1 and fig. 16) indicate that there are increased F concentrations (2,840 ppm) coincident with the REE peak anomaly that is about double the 1,450 ppm F that could be attributed to erosion from the altered scar areas upstream of the Questa deposit. Spills of mill tailings resulting from pipeline breaks could account for the REE anomalies found in the Eagle Rock Lake core providing some mechanism of enrichment could be found. URS (unpub. report, written commun., 2003) indicated a pipeline break occurred approximately 0.8 km (½ mile) upstream from Eagle Rock Lake during the 1979 flood. Fluorine concentration data from the core interval where the REE peak occurred in the sediment from Eagle Rock Lake indicate that peak F concentrations are coincident with the 1979 flood and decay exponentially with time, although not as rapidly as the REE signal from the 1979 flood event (fig. 16). Weathering of the REE from REE-bearing carbonate minerals in the fluorite would occur rapidly in the locally acidic microenvironment caused by weathering of the sulfide minerals present in the mill tailings. The REE, which have very low solubilities in SO_4^{2-}

solutions, would be immediately precipitated as $REE_2(SO_4)_3$ and transported into the Red River as colloids to be incorporated into the sediment core from Eagle Rock Lake.

Figures 15 and 16 near here

Results from Stream-Sediment Survey

The geochemical data from the NURE and from our sediment study of both premining and modern stream sediment are summarized in figures 17 and 18. Distances are plotted as river-km measured upstream from the confluence of the Red River with the Rio Grande River; the Questa open pit is at 18 – 22 river-km. The variation of Sr, Cr, V, and Mo in Red River sediment is small relative to source areas whereas Ba, Ce, and Cu, show an increase downstream of the Questa deposit. Zinc shows a broad zone of enrichment in Red River sediment downstream of the altered scar areas as well. Concentrations of all the metals shown are generally higher in the altered scar areas and in the south-flowing tributaries in the NURE data except for Zn than in Red River sediment (2002). Many of the north-flowing tributaries, which in part drain unaltered Precambrian rock south of the Red River, have metal concentrations near that in the Red River sediment or have concentrations lower than the altered scar areas. Median sediment values from Fawn Lake match well for Sr, are lower than Red River sediment for Ba, and elevated for the other six elements shown (figs 17, 18, and table 6) plotting in the field defined by data from the tributaries. Concentrations of Cu (220 ppm) plot above the range shown in fig. 18. Relative to the concentrations found in Red River sediment , median values in the post-1979 sediment of Eagle Rock Lake for Cr and V match well (fig. 17 and table 5) but for Ba and Sr are lower. Median concentrations in the sediment core of Eagle Rock Lake after 1979 (table 5) are twice that in Red River sediment for Mo, but median concentrations for Ce (260 ppm), Cu (500 ppm), and Zn (2,650 ppm) plot above the upper boundary of the diagram for these elements (fig. 18). We conclude that sediment supplied by the Red River *at low flow* in 2002 is not the same source of sediment in the post-1979 core from Eagle Rock Lake.

Tables 5 and 6, and figures 17 and 18 near here

Comparison of lake sediment geochemistry with other source materials

Sediment from Fawn Lake is not dominated by material eroded from the altered scar areas such as were sampled in Hottentot and Straight Creeks (fig. 1), but the contribution to the trace-element suite we selected is significant. Comparison of the sediment data from the altered scar areas with Fawn Lake sediment (fig. 19) shows higher concentrations of Mg, Cr, V, Cu, and Zn, and lower concentrations of Ti and Ba in sediment of Fawn Lake than in sediment from the altered scar areas. The sediment composition of the core from Fawn Lake is interpreted as a mixture of material from the upstream basin (Jackson and others, in press) and the altered scar areas.

Figure 19 near here

Comparison between post-1979 sediment from Eagle Rock Lake with the altered scar areas shows a different trend (fig. 19). Concentrations of Al, Cu, and Zn are elevated and Ti reduced in post-1979 sediment from Eagle Rock Lake relative to the concentrations in the sediment from the altered scar areas. Allen and others (1999) document the presence of an aluminum gel in the sediment of Eagle Rock Lake in the core sampled near the inlet. All three of these elements (Al, Cu, Zn) show enrichment in the lake sediment that may be explained by in-stream addition of metals by low pH groundwater (McCloskey and others, 2003). Water quality data from McCleskey and others (2003) indicate that dissolved metals enter the Red River at several places downstream from Sulfur Gulch. They document a large inflow of such ground water downstream of Bear Creek (just upstream of site 108, fig. 1).

Elevated concentrations of Mn found in the core from Eagle Rock Lake (table 2 and figs. 7 and 8) are decoupled for other trace-element distributions. These data suggest that Mn has moved within the Eagle Rock Lake core via oxidation/reduction mechanisms and is thus not a reliable indicator of source material.

Data from the composite sampling of the mine waste dumps around the open pit (Briggs and others, 2003) and from premining sediment from talus debris near and downstream of the Questa deposit (table A3) indicate that neither material alone is responsible for the geochemistry of the sediment in Eagle Rock Lake. Concentrations of Na and Ti are lower and Al, Cu, and Zn higher in the pre-1979 Eagle Rock Lake sediment than in either the premining sediment or the mine waste piles (fig. 20). Premining baseline sediment concentrations of Fe, Ti, and Ba are only somewhat higher than the mine waste piles; the other elements match reasonable well, although the range of concentrations from the premining baseline sampling is often larger than that from the mine waste. However, in the post-1979 Eagle Rock Lake sediment, concentrations of Na, Al, Cu, and Zn all plot much closer to the ranges of values found in the mine waste piles and the premining sediment (fig. 20). Only Ba shows a wider disparity.

Figure 20 near here

Discussion of Plausible Models

A major flood event occurred in the spring of 1979 on the Red River (table 1). Photographs of the flood (fig. 21) show the magnitude of this event. Major changes took place in the floodplain of the Red River. The historical record indicates that there was a major pipeline break 0.8 km upstream from Eagle Rock Lake during the flood. Following the flood, the floodplain of the Red River was graded to remove obstacles to flow introduced into the channel (USDA Forest Service Questa Ranger Station, 2002). Crawler tractor tracks still persist in the riparian zone in places above high-water level on the Red River floodplain. This activity has hidden the source of the material added to the Red River that would account for the geochemistry of the post-1979 sediment in Eagle Rock Lake. We cannot distinguish the source of this material from existing data. However, the source could be readily identified should funds become available. At low flow and during drought years, sediment supplied to Eagle Rock Lake appears to be very similar to the pre-1979 source, which are the Precambrian rocks exposed in the rest of the Red River valley watershed. However, in wet years, we hypothesize that material deposited on the low terraces in the Red River floodplain and was redistributed along these terraces by the crawler tractor work following the 1979 flood may be the source of sediment deposited in Eagle Rock Lake during these high-flow periods.

Figure 21 near here

Summary and Conclusions

Geochemical data from the study of cores in Fawn and Eagle Rock Lakes has provided a continuous record of sedimentation from their inception in 1961. Radiometric dating using ^{137}Cs confirms the historical date provided by the New Mexico Dept. of Highways on the inception of the lakes and demonstrates that sedimentation has been continuous since that time. The geochemical data from Fawn Lake provide a very reliable and continuous record of geochemical background concentrations over the period from 1961-2002. The sedimentary record from the Eagle Rock Lake core indicates very similar sedimentary history from its inception until 1979. Concentrations of Mo, Co, Ni, Cu, and Zn increased during the period from 1963 – 1967, which we interpret as the period when the site for the open pit at Questa was being prepared and work on the open pit began. Other geochemical anomalies shown by rare earth element (REE) and fluorine concentrations in the sediment core are correlated with known breaks in the pipeline that transports mill tailings to the repository below the town of Questa. REE are present in carbonate minerals in the hydrothermal megabreccia in the ore deposit. Enrichment of the REE by accelerated weathering is required to explain the anomalies in sediment from Eagle Rock Lake. The sedimentary record Eagle Rock Lake changed substantially in 1979 with large increases in concentration for many major elements and metals in sediment in Eagle Rock Lake. This change in source material was enormous; it has dominated the sediment supplied by the Red River to Eagle Rock Lake for more than 2 decades. We interpret these data to indicate that a new source of sediment may have been impounded on the low terraces of Red River downstream from Fawn Lake and redistributed by the channelization that occurred following the 1979 flood-of-record. Although both mine waste and premining background sediment from altered areas around the Questa porphyry Mo deposit have the appropriate compositions to be potential sources of this new sediment, existing data are not sufficient to implicate or refute either one. Given the very large disturbance represented by the mine-waste piles at the open pit site, erosion of the mine wastes must be considered a very plausible source of this sediment during the 1979 flood-of-record despite the presence of large berms built by Molycorp to prevent such erosion.

References Cited

Briggs, P.H., 1996, Forty elements by inductively coupled plasma-atomic emission spectrometry: *in* Arbogast, B.F., ed., Analytical methods manual of the Mineral Resource Surveys Program, U.S. Geological Survey: U.S. Geological Survey Open-File Report 96-525, pp. 77-94.

Briggs, P.H., Sutley, S.J., and Livo, K.E., Questa baseline and pre-mining ground water investigation: 11. Geochemistry of composited material from alteration scars and mine-waste piles: U.S. Geological Survey Open-File Report 03-458, 16 p.

Carpenter, R.H., 1968, Geology and ore deposits of the Questa molybdenum mine area, Taos County, New Mexico, *in* Ridge, J.D., ed., Ore deposit of the United States, 1933-1967 (Graton Sales volume): New York, American Institute of Mining Metallurgical and Petroleum Engineers, v. 2, p. 1328-1350.

Carten, R.B., White, W.H., and Stein, H.J., 1993, High-grade granite-related molybdenum systems: Classification and origin: Geological Association of Canada Special Paper 40. p. 521-544.

Church, S.E., Fey, D.L., and Blair, Robert, 2000, Pre-mining bed sediment geochemical baseline in the Animas River watershed, southwestern Colorado: ICARD 2000: Proceedings from the Fifth International Conference on Acid Rock Drainage, Lakewood, Society for Mining, Metallurgy, and Exploration, Inc., v. 1, p. 499-512.

Czamanske, G.K., Foland, K.A., Kubacher, F.A., and Allen, J.C., 1990, The $^{40}Ar/^{39}Ar$ chronology of caldera formation, intrusive activity, and Mo-ore deposition near Questa, New Mexico, *in* Bauer, P.W., Lucas, S.G., Mawer, C.K., and McIntosh, W.C., eds.: New Mexico Geological Society Guidebook, 41st Field Conference, Southern Sangre de Cristo Mountains, p. 355-358.

Fey, D.L., Unruh, D.M., and Church, S.E., 1999, Chemical data and lead isotopic compositions in stream sediment samples from the Boulder River watershed, Jefferson County, Montana: U.S. Geological Survey Open-File Report 99-575, 147 p.

Fortescue, J.A.C., 1992, Landscape geochemistry: retrospect and prospect—1990: Applied Geochemistry, v. 7, p. 1-53.

Johnson, C.M., and Lipman, P.W., 1988, Origin of metaluminous and alkaline volcanic rocks of the Latir volcanic field, northern Rio Grande rift, New Mexico: Contributions Mineralogy and Petrology, v. 100, p. 107-128.

Johnson, C.M., Czamanske, G.K., and Lipman, P.W., 1989, Geochemistry of intrusive rocks associated with the Latir volcanic field, New Mexico, and contrasts between evolution of plutonic and volcanic rocks: Contributions Mineralogy and Petrology, v. 103, p. 90-109.

Johnson, C.M., Lipman, P.W., and Czamanske, G.K., 1990, H, O, Sr, Nd, and Pb isotope geochemistry of the Latir volcanic field and cogenetic intrusions, New Mexico, and relations between evolution of a continental magmatic center and modifications of the lithosphere: Contributions Mineralogy and Petrology, v. 104, p. 99-124.

Laughlin, A.W., Rehrig, W.A., and Mauger, R.L., 1969, K-Ar chronology and sulfur and strontium isotope ratios at the Questa mine, New Mexico: Economic Geology, v. 64, p. 903-909.

Leonardson, R.W., Dunlop, G., Starquist, V.L., Bratton, G.P., Meyer, J.W., Osborne, L.W., Atkin, S.A., Molling, P.A., Moore, R.F., and Olmore, S.D., 1983, Preliminary geology and molybdenum deposits at Questa, New Mexico, *in* Changes with time and tectonics: Society of Exploration Geologists, Denver Region, Symposium Proceedings, p. 151-155.

Lipman, P.W., Bowman, H.R., Knight, Roy, Millard, H.T., Jr., Pallister, J.S., Street, K. Wollenberg, H., and Zielinski, R.A., 1982, Instrumental neutron activation of Cenozoic volcanic rocks, phenochrysts, and associated intrusions form the southern Rocky Mountains and adjacent areas: U.S. Geological Survey Open-File Report 82-1069, 1 sheet.

Lipman, P.W., 1981, Volcanic-tectonic setting of Tertiary ore deposits, southern Rocky Mountains: Arizona Geologic Society Digest, v. 14, p. 199-214.

Lipman, P.W., 1983, The Miocene Questa caldera, northern New Mexico—Relation to batholith emplacement and associated molybdenum mineralization, *in* Changes with time and tectonics: Society of Exploration Geologists, Denver Region, Symposium Proceedings, p. 133-149.

Lipman, P.W., 1988, Evolution of silicic magma in the upper crust—the Mid-Tertiary Latir volcanic field and its cogenetic granitic batholith, northern New Mexico, U.S.A.: Transactions of the Royal Society of Edinburgh: Earth Sciences, v. 79, p. 265-288.

Lipman, P.W., and Reed, J.C. Jr., 1989, Geologic map of the Latir volcanic field and adjacent areas, northern New Mexico: U. S. Geological Survey Miscellaneous Investigations Series Map I-1907, scale 1:48,000.

Lipman, P.W., Mehnert, H.H., and Naeser, C.M., 1986, Evolution of the Latir volcanic field, northern New Mexico, and its relation to the Rio Grande rift, as indicated by potassium-argon and fission tract dating: Journal of Geophysical Research, v. 91, p. 6329-6345.

Livo, K.E., and Clark, R.N., 2002, Mapped minerals at Questa New Mexico, using Airborne Visible-Infrared Imaging Spectrometer (AVIRIS) data—Preliminary report: U.S. Geological Survey Open-File Report 02-0026, 13 p.

Ludington, S.D., Plumlee, G., Caine, J., Bove, D.J., Holloway, J., and Livo, E., 2004, Questa baseline and pre-mining ground-water quality investigation. 10. Geologic influences on ground and surface waters in the lower Red River watershed, New Mexico: U.S. Geological Survey Open-File Report 04-xxx, yy p.

McCleskey, R.B., Nordstrom D.K., Steiger, J.I., Kimball, B.A., and Verplanck, P.L., 2003, Questa baseline and pre-mining ground-water quality investigation. 2. Low-flow (2001) and snowmelt (2002) synoptic/tracer water chemistry for the Red River, New Mexico: U.S. Geological Survey Open-File Report 03-148, 166 p.

Meyer, J. and Leonardson, R.W., 1990, Tectonic, hydrothermal and geomorphic controls on alteration scar formation near Questa, New Mexico, *in* Bauer, P.W., Lucas, S.G., Mawer, C.K., and McIntosh, W.C., eds.: New Mexico Geological Society Guidebook, 41st Field Conference, Southern Sangre de Cristo Mountains, New Mexico, p. 417-422.

Ross, P.S., Jébrak, Michel, and Walker, B.M., 2002, Discharge of hydrothermal fluids from a magma chamber and concomitant formation of a stratified breccia zone at the Questa porphyry molybdenum deposit, New Mexico: Economic Geology, v. 97, p. 1679-1699.

Sutley, Stephen, Ludington, S.D., Billings, Patty, and Jones, David, 1983, Chemical analyses and statistical summary for samples of minus-200-mesh stream sediment, magnetic, and nonmagnetic heavy-mineral concentrates from the Latir Peak and Wheeler Peak wildernesses and the Columbine-Hondo wilderness study area, Taos County, New Mexico: U.S. Geological Survey Open-File Report 83-360, 36 p., 1 plate, scale 1:50:000.

Uranium Resource Evaluation Project (NURE), 1981, Hydrogeochemical and stream sediment reconnaissance basic data for Raton quadrangle, New Mexico: Union Carbide Corporation, Nuclear Division, Oak Ridge Gaseous Diffusion Plant, Oak Ridge, Tenn., K/UR-343, U.S. Department of Energy, Grand Junction, Colo., GJBX-358(81), 185 p.

Wedepohl, K.H., ed., 1970, Handbook of Geochemistry, v. II-2, Springer-Verlag, New York, variously paginated.

Appendix

Table A1. Analytical data from core from Eagle Rock Lake, Questa study area, New Mexico.

Table A2. Analytical data from core from Fawn Lake, Questa study area, New Mexico.

Table A3. Analytical data from debris fans, modern and background sediment, and tailings spill samples, Questa study area, New Mexico.

Figure captions

Figure 1. Topographic map of study area showing locations of alteration scars, debris fans, and mineral deposits (after Ludington and others, 2004), and sediment sample localities (tables A1-A3). Outline of the Questa open pit is shown as a dashed line. Map projection is UTM, zone 13N; geographic coordinate system is North American datum 1927. One additional stream-sediment sample (not shown) was collected at the fish hatchery downstream from Questa near the confluence of Red River with the Rio Grande River. Sample localities of mill tailings spills and debris fans are not shown.

Figure 2. Photograph of the USGS pontoon boat used to core the sediment in Fawn and Eagle Rock Lakes. Anchors were deployed from each corner and the core driven through an opening in the deck. Core was then pulled using a hoist attached to the tower (assembly in progress). Core was sectioned on site, the samples placed in plastic bags, and they were shipped to laboratory for processing. Photograph taken at Eagle Rock Lake dam, June 2002 by Philip Verplanck.

Figure 3. Plot of monthly discharge (in ft^3/sec or cfs) versus time (1960-2002) for the gage at Questa, New Mexico (http://nm.waterdata.usgs.gov/nwis). The flood of record (74 years) occurred in spring, 1979 (table 1).

Figure 4. Plot of ^{137}Cs concentration versus depth (cm) in the Eagle Rock Lake (ERL) and Fawn Lake (FL) cores. Well-defined peaks in ^{137}Cs activity occur at slightly different depths in the two lakes, but both are quit close to the bottom of the core where we encountered fragmented bedrock. Since the lakes originated as borrow pits dug to complete the paving of NM Highway 38 from Questa to Red River in 1961, we interpret the differences in sedimentation rates at the bottom of the core to reflect the fact that roadwork began at Questa and moved upstream. Head gates were installed by the local irrigation company, which subsequently limited flow through and thus sediment accumulation in the two lakes.

Figure 5. Plot of the sedimentation rate used for both the Eagle Rock (ERL) and Fawn Lake (FL) cores. The depth of the 1963 ^{137}Cs peak and the geochemical data from the 1979 flood-of-record were used to construct the sedimentation model.

Figure 6. Plot of concentrations of the major elements Na, K, Mg, Ca, Al, and Si, expressed as oxides, versus time as determined from the sedimentation rate curve (fig. 5) for the cores from Fawn Lake

(FL) and Eagle Rock Lake (ERL). Values for the average monthly discharge measured at the Questa gage (08265000) are shown to facilitate correlation of element concentrations with the hydrograph.

Figure 7. Plot of concentrations of the major elements Fe and Ti, expressed as oxides, and minor and trace elements Mn, V, Cr, and Pb versus time as determined from the sedimentation rate curve (fig. 5) for the cores from Fawn Lake (FL) and Eagle Rock Lake (ERL). Values for the average monthly discharge measured at the Questa gage (08265000) are shown to facilitate correlation of element concentrations with the hydrograph. Crustal abundance values (Fortescue, 1992) of Mn (1,060 ppm), V (136 ppm), Cr (122 ppm), and Pb (13 ppm) are indicated by the arrow on the concentration axis of the figures where within range.

Figure 8. Plot of concentrations of the trace elements Co, Ni, Cu, Mo, Zn, and Cd versus time as determined from the sedimentation rate curve (fig. 5) for the cores from Fawn Lake (FL) and Eagle Rock Lake (ERL). Values for the average monthly discharge measured at the Questa gage (08265000) are shown to facilitate correlation of element concentrations with the hydrograph. Crustal abundance values (Fortescue, 1992) of Co (29 ppm), Ni (99 ppm), Cu (68 ppm), Mo (1.2 ppm), Zn (76 ppm), and Cd (0.16 ppm) are indicated by the arrow on the concentration axis of the figures where within range.

Figure 9. Plot of concentrations of the lithophile trace elements Li, Be, Sr, Ba, and P (expressed as an oxide) versus time as determined from the sedimentation rate curve (fig. 5) for the cores from Fawn Lake (FL) and Eagle Rock Lake (ERL). Values for the average monthly discharge measured at the Questa gage (08265000) are shown to facilitate correlation of element concentrations with the hydrograph. Crustal abundance values (Fortescue, 1992) of Li (18 ppm), Be (2.0 ppm), Sr (384 ppm), Ba (390 ppm), and P (1,120 ppm) are indicated by the arrow on the concentration axis of the figures where within range.

Figure 10. Plot of concentrations of the rare earth elements La, Ce, Nd, and Yb, and Y versus time as determined from the sedimentation rate curve (fig. 5) for the cores from Fawn Lake (FL) and Eagle Rock Lake (ERL). Values for the average monthly discharge measured at the Questa gage (08265000) are shown to facilitate correlation of element concentrations with the hydrograph. Crustal abundance values (Fortescue, 1992) of La (34.6 ppm), Ce (66.4 ppm), Nd (39.6 ppm), Yb (3.1 ppm), and Y (31 ppm) are indicated by the arrow on the concentration axis of the figures where within range.

Figure 11. Box plot comparing the geochemical data from:

A. Major element data (Na_2O, MgO, FeO, Al_2O_3, and TiO_2), Fawn Lake core (table A2), for the pre-1979 ($n = 20$) and the post-1979 ($n = 30$) intervals,

B. Trace element data (Ba, Sr, Cr, V, Cu, Zn), Fawn Lake core (table A2), for the pre-1979 ($n = 20$) and the post-1979 ($n = 30$) intervals,

C. Major element data (Na_2O, MgO, FeO, Al_2O_3, and TiO_2), Eagle Rock Lake core (table A1), for the pre-1979 ($n = 24$; ERL pre-1979) and the post-1979 ($n = 30$; ERL post-1979) intervals,

D. Trace element data (Ba, Sr, Cr, V, Cu, Zn), Eagle Rock Lake core (table A1), for the pre-1979 ($n = 24$; ERL pre-1979) and the post-1979 ($n = 30$; ERL post-1979) intervals,

E. Major element data (Na_2O, MgO, FeO, Al_2O_3, and TiO_2), Fawn Lake for the entire core (table A2, $n = 50$) and the Eagle Rock Lake core for the pre-1979 (table A1, $n = 24$) intervals, and

F. Trace element data (Ba, Sr, Cr, V, Cu, Zn), Fawn Lake for the entire core (table A2, $n = 50$) and the Eagle Rock Lake core for the pre-1979 (table A1, $n = 24$) intervals.

The median value for each element is bracketed by the 25^{th} and 75^{th} percentile of the data forming the box and the 10^{th} and 90^{th} percentiles are indicated by the lines above and below the box.

Figure 12. Photographs of the 1981 pipeline break (A) and cleanup by Molycorp (B) at the USDA Forest Service Goat Hill Campground, winter of 1981. (Photos from USDA Forest Service files provided by George Long, Questa Ranger Station, New Mexico, 2003).

Figure 13. Plot of chondrite-normalized REE patterns for volcanic (A) and plutonic (B) rocks from the study area. REE data from Eagle Rock Lake are the minimum and maximum values recovered from the sediment core (table A1) whereas the REE data from Fawn Lake is from the sample with the median value for cerium (table A2). REE data for the rocks are from Lipman and others (1980) and from Johnson and others (1989).

Figure 14. Photographs of four fluorite samples from the D ore body (samples supplied by Megan Jackson, Molycorp, 2003). Analytical data are in table 4.

A. Sample QF-2 is a coarsely crystalline fluorite sample, possibly from a vein(?). The green mineral is fluorite, white mineral is calcite, and there were minor amounts of molybdenite visible in the speciman. Calcite and fluorite separates were hand-picked and analyzed from this sample.

B. Sample QF-3 is laminated with more calcite (white) than fluorite (green). There were minor amounts of molybdenite visible in the speciman. Grain size ranged from 2 - 4 mm. Calcite and fluorite separates were hand-picked and analyzed.

C. Sample QF-4 is a coarse-grained mixture of calcite (white), fluorite (green), and molybdenite (gray) with minor amounts of pyrite (brass colored). Fluorite accumulations ranged in size from about 2 mm to 1 cm. Calcite and fluorite separates were hand-picked and analyzed.

D. Sample QF-5 is a medium to coarse-grained mixture of calcite (white), fluorite (green) and molybdenite (gray) with minor amounts of pyrite (brass colored). Fluorite accumulations ranged in size from about 2 mm to 1 cm. Sample contains wall rock inclusion on the lower right. No mineral separates were picked from this sample.

Figure 15. Electron backscatter photomicrograph taken in SEM (Sharon Diehl, analyst, 2003). REE-bearing phosphate, carbonate, and sulfate (not shown) minerals were identified as small inclusions in the fluorite from the D ore body, Questa mine.

Figure 16. Plot of concentration of the rare earth element cerium in the cores from Fawn Lake (FL) and Eagle Rock Lake (ERL), and fluorine from the Eagle Rock Lake core (table A1) versus time as determined from the sedimentation rate curves (fig. 5).

Figure 17. Plots of the concentration of trace elements, Ba, Sr, Cr, and V, in sediment from the Red River (table A3), sediment from tributary streams (table A3) and from the 1976 NURE study (NURE, 1981). The concentrations of the elements Sr, Cr, and V do not change significantly in sediment of the Red River as it flows past the Questa open pit (18 - 22 km), however, Ba is significantly enriched in Red River sediment downstream of the mine site.

Figure 18. Plots of the concentration of trace elements, Ce, Mo, Cu, and Zn, in sediment from the Red River (table A3), sediment from tributary streams (table A3) and from the 1976 NURE study (NURE, 1981). The concentrations of all four of the elements are enriched in sediment of the Red River before it reaches the Questa open pit (18 - 22 km). Concentrations of these metals in sediment from many of the tributaries are elevated above that of the Red River sediment.

Figure 19. Box plot comparing the geochemical data from:

A. Major element data (Na_2O, MgO, FeO, Al_2O_3, and TiO_2), Fawn Lake core (table A2, $n = 50$) and alteration scars (table A3, $n > 30$, these are composite samples),

B. Trace element data (Ba, Sr, Cr, V, Cu, Zn), Fawn Lake core (table A2, $n = 50$) and alteration scars (table A3, $n > 30$, these are composite samples),

C. Major element data (Na_2O, MgO, FeO, Al_2O_3, and TiO_2), Eagle Rock Lake core, post-1979 interval (ERL-post-1979; table A1, $n = 30$) and alteration scars (table A3, $n > 30$, these are composite samples), and

D. Trace element data (Ba, Sr, Cr, V, Cu, Zn), Eagle Rock Lake core, post-1979 interval (ERL-post-1979; table A1, $n = 30$) and alteration scars (table A3, $n > 30$, these are composite samples).

The median value for each element is bracketed by the 25^{th} and 75^{th} percentile of the data forming the box and the 10^{th} and 90^{th} percentiles are indicated by the lines above and below the box.

Figure 20. Box plot comparing the geochemical data from:

A. Major element data (Na_2O, MgO, FeO, Al_2O_3, and TiO_2), pre-1979 interval, Eagle Rock Lake core (ERL-pre-1979; table A1, $n = 24$), the mine-waste piles (Briggs and others, 2003; $n > 30$, these are composite samples), and premining sediment (table A3, $n > 30$, these are composite samples),

B. Trace element data (Ba, Sr, Cr, V, Cu, Zn), pre-1979 interval, Eagle Rock Lake core (ERL-pre-1979; table A1, $n = 24$), the mine-waste piles (Briggs and others, 2003; $n > 30$, these are composite samples), and premining sediment (table A3, $n > 30$, these are composite samples),

C. Major element data (Na_2O, MgO, FeO, Al_2O_3, and TiO_2), post-1979 interval, Eagle Rock Lake core (ERL-post-1979; table A1, $n = 30$), the mine-waste piles (Briggs and others, 2003; $n > 30$, these are composite samples), and premining sediment (table A3, $n > 30$, these are composite samples), and

D. Trace element data (Ba, Sr, Cr, V, Cu, Zn), post-1979 interval, Eagle Rock Lake core (ERL-post-1979; table A1, $n = 30$), the mine-waste piles (Briggs and others, 2003; $n > 30$, these are composite samples), and premining sediment (table A3, $n > 30$, these are composite samples).

The median value for each element is bracketed by the 25^{th} and 75^{th} percentile of the data forming the box and the 10^{th} and 90^{th} percentiles are indicated by the lines above and below the box.

Figure 21. Photographs of the Red River at flood stage, spring of 1979. (Photos from USDA Forest Service files provided by George Long, Questa Ranger Station, New Mexico, 2003). Both the 1979 flood-of-record (natural) and the subsequent channelizing of the Red River by the Caterpiller (anthropogenic) were significant agents of change associated with this flood.

Table 1. Mean Daily Peak flow at Questa gage (08265000), New Mexico

Year	Period	Mean Daily Peak Flow Rate	No. of days flow exceeded 300 cfs
1965	June 18 - 20	320	3
1973	June 14 - 15	314	2
1979	May 20 - July 3	557	44
1983	May 30 - June 2	332	4
1984	May 23 - May 28	372	6
1985	May 10 - 11	319	2
1985	June 9 - June 13	322	5
1986	June 8 - June 9	325	2
1991	May 21 - May 24	469	4
1993	May 28	301	1
1994	May 16 - June 8	399	21
1995	June 14 - June 23	359	10
1997	June 2 - June 8	347	7

Table 3. Anomalies of metals directly associated with the Questa porphyry molybdenum deposit that also occur in the core from Eagle Rock Lake, Red River valley, New Mexico

Molybdenum	Copper-Zinc	Cobalt-Nickel	Rare Earth Elements
1963 - 67	1963 - 67	1966 - 67	
			1967 – 1969
1969 - 75			
	1972 - 73	1975	
1979 - 82	1979		
		1981 - 82	1978 - 83
	1987 - 90		
		1989 - 92	1988 - 89
	1994		1994
		1998 - 99	1998 - 99
	2002	2002	

Table 2. Summary of the geochemical data from cores in Fawn Lake and Eagle Rock Lakes, Red River valley, New Mexico

[Filled squares indicate times where peaks in concentration were identified.]

Fawn Lake

	Silicates								Oxides			Sulfides							Accessory minerals									
Year	Na	K	Mg	Ca	Al	Si	Fe	Mn	Ti	V	Cr	Pb	Co	Ni	Mo	Cu	Zn	Cd	Li	Be	Sr	Ba	P	La	Ce	Nd	Yb	Y
1961	X					X																						
1962	X																		X									
1963		X						X	X			X											X					
1964		X			X				X			X											X					
1965		X								X	X										X		X					
1966		X								X	X	X									X		X					
1967	X					X			X	X	X	X				X	X					X	X					
1968	X					X			X		X					X	X											
1969	X										X					X	X											
1970	X										X					X	X											
1971	X						X									X	X											
1972	X			X			X					X	X	X	X	X	X											
1973						X	X																					
1974											X	X																
1975		X							X	X	X																	
1976	X			X					X	X	X										X							
1977	X					X															X							
1978										X	X																	
1979	X	X	X		X		X	X	X	X	X	X		X	X	X	X		X	X	X	X	X	X	X	X		X
1980											X																	
1981				X																								
1982		X		X	X					X		X									X		X					
1983	X	X		X						X		X																
1984	X			X		X			X																			
1985																												
1986				X																								
1987	X			X							X										X							
1988	X			X			X							X		X					X							
1989				X		X	X						X	X		X	X	X			X		X				X	X
1990				X		X	X						X	X		X	X											X
1991						X	X							X	X	X												
1992						X	X								X	X												
1993	X		X				X			X	X	X			X						X		X					
1994		X	X				X			X	X	X									X							
1995	X		X				X		X	X							X		X									
1996	X					X											X											
1997		X							X			X									X		X					
1998	X					X			X			X					X				X		X					
1999	X																											
2000		X																					X					
2001		X					X					X											X					
2002						X		X									X											

Eagle Rock Lake

	Silicates								Oxides			Sulfides							Accessory minerals									
Year	Na	K	Mg	Ca	Al	Si	Fe	Mn	Ti	V	Cr	Pb	Co	Ni	Mo	Cu	Zn	Cd	Li	Be	Sr	Ba	P	La	Ce	Nd	Yb	Y
1961	X					X																						
1962	X		X			X								X			X					X						
1963			X				X		X	X		X		X	X	X	X		X	X			X					X
1964			X		X					X		X		X	X	X	X		X	X	X		X					X
1965			X		X				X	X	X	X		X	X	X	X		X	X	X		X					X
1966		X	X		X					X		X	X	X	X	X	X	X	X	X			X					X
1967				X			X					X	X	X	X	X	X	X		X			X	X	X	X		X
1968				X		X			X								X				X	X		X	X	X		X
1969			X	X					X						X							X		X	X	X		X
1970		X	X				X			X	X	X			X				X						X			X
1971		X	X							X	X	X			X				X									
1972			X									X			X	X	X	X	X									
1973															X	X	X	X	X				X					X
1974	X						X								X	X			X									
1975						X	X						X	X	X		X	X	X				X			X	X	X
1976		X	X		X				X		X	X					X				X		X				X	X
1977		X							X		X	X							X		X	X	X					
1978												X	X	X	X		X		X				X	X	X	X	X	X
1979					X										X	X	X	X		X		X		X	X	X	X	X
1980														X	X	X	X		X	X		X		X	X	X	X	X
1981							X						X	X	X	X	X	X		X				X	X	X	X	X
1982							X						X	X	X	X	X	X		X				X	X	X	X	X
1983														X			X			X				X	X	X	X	X
1984																	X								X			X
1985		X							X	X		X					X				X							
1986		X																	X									
1987																X	X		X									
1988													X	X		X	X		X								X	X
1989										X			X	X		X	X		X								X	X
1990													X	X		X	X		X									
1991						X							X	X			X		X									
1992													X	X			X		X									
1993														X			X		X									
1994														X		X	X			X		X		X	X	X	X	X
1995															X						X	X	X					
1996		X	X				X		X	X	X	X							X		X							
1997							X										X		X					X		X		X
1998						X								X		X		X		X					X		X	
1999	X	X	X								X		X								X		X					
2000		X	X				X		X	X																		
2001							X					X																
2002	X					X							X	X		X	X	X	X	X				X	X	X	X	X

Table 4. Analyses of fluorite from megabreccia, Queste molybdenum mine area, Red River valley, New Mexico

Sample	Mineral Phase		Ca %	Mg %	Na %	K %	Al %	P %	Mn ppm	La ppm	Ce ppm	Nd ppm	Eu ppm	Yb ppm	Y ppm	Li ppm	Be ppm	Sr ppm	Ba ppm
										Rare Earth Elements									
QSGF-1																			
	Mixed phases	leach	19.5	0.018	0.013	0.150	0.165	0.005	17	6	6	7	<2	<1	5	2	<1	39	6
	Mixed phases	residue	22.4	<0.005	<0.005	<0.01	0.025	<0.005	<2	7	10	10	<2	<1	48	3	<1	41	<1
	Mixed phases	sum	41.9	0.018	0.013	0.150	0.190	0.005	17	13	15	17	<2	<1	53	5	<1	81	6
QF-2--Carbonate phase																			
	Carbonate (white phase)	leach	24.4	0.095	0.200	3.81	3.65	0.009	31	39	63	29	<2	<1	31	11	2	65	390
	Carbonate (white phase)	residue	0.8	0.006	0.011	0.20	0.22	<0.005	2	18	27	9	<2	<1	4	8	<1	4	27
	Carbonate (white phase)	sum	25.2	0.100	0.211	4.01	3.87	0.009	32	56	90	38	<2	<1	36	19	2	70	420
QF-2--Carbonate phase (replicate)																			
	Carbonate (white phase)	leach	25.1	0.094	0.199	3.85	3.66	0.009	30	44	71	32	<2	<1	33	11	2	67	390
	Carbonate (white phase)	residue	0.2	0.005	0.008	0.15	0.19	<0.005	2	14	21	7	<2	<1	3	8	<1	3	22
	Carbonate (white phase)	sum	25.3	0.100	0.207	4.00	3.85	0.009	32	58	92	39	<2	<1	36	19	2	71	410
QF-2--Fluorite																			
	Fluorite (green phase)	leach	4.9	0.003	<0.005	0.015	0.010	<0.005	16	13	20	11	<2	<1	2	<1	<1	7	<1
	Fluorite (green phase)	residue	33.1	<0.005	<0.005	<0.01	0.032	0.005	<2	60	95	41	<2	<1	39	7	<1	45	24
	Fluorite (green phase)	sum	38.0	0.003	<0.005	0.015	0.042	0.005	16	72	110	52	<2	<1	41	7	<1	52	24
QF-3--Carbonate phase																			
	Carbonate (white phase)	leach	27.9	0.052	0.001	<0.01	0.017	<0.005	2830	34	52	24	<2	<1	6	<1	<1	170	<1
	Carbonate (white phase)	residue	8.9	<0.005	<0.005	<0.01	0.036	0.010	4	60	98	40	<2	<1	28	16	<1	16	22
	Carbonate (white phase)	sum	36.9	0.052	0.001	<0.01	0.053	0.010	2830	95	150	63	<2	<1	34	16	<1	190	22
QF-3--Fluorite phase																			
	Fluorite (green phase)	leach	13.9	0.013	0.001	0.013	0.027	0.011	240	170	280	120	2	<1	9	<1	<1	49	<1
	Fluorite (green phase)	residue	33.4	<0.005	0.017	<0.01	0.027	0.010	2	190	320	130	3	5	120	6	<1	75	62
	Fluorite (green phase)	sum	47.3	0.013	0.018	0.013	0.054	0.022	240	360	600	250	5	5	130	6	<1	120	62
QF-4--Carbonate phase																			
	Carbonate (white phase)	leach	17.5	0.087	0.005	0.018	0.072	0.023	2150	58	97	42	<2	2	27	1	<1	120	3
	Carbonate (white phase)	residue	1.0	<0.005	0.006	<0.01	0.060	<0.005	3	18	28	11	<2	<1	3	31	<1	4	5
	Carbonate (white phase)	sum	18.6	0.087	0.011	0.018	0.132	0.023	2150	76	130	53	<2	2	30	32	<1	120	8
QF-4--Fluorite phase																			
	Fluorite (green phase)	leach	7.2	0.015	<0.005	0.014	0.014	<0.005	270	140	240	100	2	<1	16	<1	<1	150	53
	Fluorite (green phase)	residue	38.0	<0.005	<0.005	<0.01	0.039	0.017	<2	270	470	200	4	5	130	6	<1	88	94
	Fluorite (green phase)	sum	45.2	0.015	<0.005	0.014	0.054	0.017	270	410	710	300	6	5	150	6	<1	240	150
QF-5																			
	Mixed phases	leach	4.2	0.007	0.007	0.032	0.065	<0.005	24	51	74	21	<2	<1	2	2	<1	24	4
	Mixed phases	residue	19.4	<0.005	0.005	0.011	0.111	0.013	<2	320	540	220	4	2	79	43	<1	53	110
	Mixed phases	sum	23.6	0.007	0.012	0.043	0.176	0.013	24	370	610	240	4	2	81	46	<1	77	110

Table 5. Statistics for post-1979 concentrations of major and trace elements in sediment from Eagle Rock Lake core, Red River valley, New Mexico

	Na_2O %	K_2O %	MgO %	CaO %	Al_2O_3 %	FeO %	TiO_2 %	P_2O_5 %	SiO_2 % (diff)	Mn ppm	V ppm
Minimum	0.32	1.7	1.1	0.46	18.9	3.5	0.10	0.32	61.7	420	52
Maximum	0.51	4.5	2.0	0.98	26.5	8.0	0.40	0.48	69.8	2700	100
Median	0.42	2.6	1.5	0.76	22.7	5.7	0.18	0.37	66.5	1950	74
Mean	0.41	2.8	1.5	0.72	22.0	5.9	0.20	0.39	66.1	1730	74
Standard Deviation	0.05	0.8	0.3	0.17	1.5	1.1	0.07	0.05	1.9	679	14

	Cr ppm	Co ppm	Ni ppm	Mo ppm	Cu ppm	Zn ppm	Pb ppm	Li ppm	Sr ppm	Ba ppm	La ppm	Ce ppm	Y ppm
Minimum	39	8	33	16	62	240	97	26	110	200	65	110	16
Maximum	79	220	470	96	820	4600	250	51	370	820	350	680	320
Median	56	77	210	26	500	2650	150	40	170	715	130	260	140
Mean	57	81	212	36	466	2390	151	40	191	640	157	305	153
Standard Deviation	10	51	102	23	182	972	38	7	69	196	84	167	78

Table 6. Statistics for trace-element concentrations in sediment from Fawn Lake core, Red River valley, New Mexico

	Mn ppm	V ppm	Cr ppm	Co ppm	Ni ppm	Mo ppm	Cu ppm	Zn ppm	Pb ppm	Li ppm	Sr ppm	Ba ppm	Ce ppm	Y ppm
Minimum	410	78	62	3	20	12	77	140	100	24	180	110	72	14
Maximum	880	170	150	72	140	48	410	1200	320	50	360	770	150	45
Median	560	100	81	22	57	24	220	485	200	33	220	220	94	24
Mean	551	101	81	23	58	26	218	487	205	32	222	243	92	25
Standard Deviation	91.9	13.3	13.0	12.8	22.9	9.0	66.3	199.6	55.0	3.5	32.1	122.4	10.6	6.3

Table A1. Analytical data from the core from Eagle Rock Lake, lower Red River, New Mexico.

[Depth of each subsample, in cm; Cs-137 activity of selected subsamples (dpm/g, dissentigrations per minute per gram); the solid fraction of each sample (dried sample compared to wet sample); and elemental concentrations in weight percent for major elements, parts per million (ppm) dry weight; --, not analyzed. Subsample 02QNM101Lq is missing, due to loss during preparation. Elemental analyses by ICP-AES following complete mixed-acid digestion (Briggs, 1996); elements analyzed but not detected (Ag, Bi, Th) not reported. Locality coordinates: 36.70362 degrees North latitude; 105.57329 degrees West longitude.]

Field Number	Depth (cm)	Cs-137 Activity (dpm/g)	Solid Fraction	Al %	Ca %	Fe %	K %	Mg %	Na %	P %	Ti %	As ppm	Ba ppm	Be ppm	Cd ppm	Ce ppm	Co ppm	Cr ppm	Cu ppm	Eu ppm	F ppm	Ga ppm	Ho ppm	La ppm	Li ppm	Mn ppm	Mo ppm	Nb ppm	Nd ppm	Ni ppm	Pb ppm	Sc ppm	Sn ppm	Sr ppm	V ppm	Y ppm	Yb ppm	Zn ppm
02QNM101La	0.5	--	0.23	12	0.62	4.2	2.1	0.86	0.38	0.16	0.12	16	780	14	12	280	85	54	530	10	--	22	6	140	49	2100	26	49	240	240	130	10	6	170	70	170	9	2700
02QNM101Lb	1.5	--	0.23	12	0.40	5.4	3.2	1.0	0.26	0.18	0.15	14	300	9	6	170	31	62	300	5	--	26	<4	94	35	2200	25	48	130	110	200	9	<5	240	82	88	5	1500
02QNM101Lc	2.5	--	0.34	11	0.35	5.9	3.7	1.2	0.31	0.20	0.21	17	200	5	4	130	14	74	120	2	--	31	<4	76	30	1100	22	63	76	56	180	11	5	320	99	34	2	610
02QNM101Ld	3.5	--	0.42	11	0.34	5.6	3.7	1.2	0.35	0.21	0.24	20	470	3	2	110	8	79	62	<2	--	33	<4	65	26	420	16	76	55	33	150	11	<5	370	100	16	1	240
02QNM101Le	4.5	--	0.25	12	0.41	4.4	2.7	1.0	0.30	0.18	0.12	11	820	10	7	190	55	64	390	6	--	25	<4	99	32	560	17	63	150	150	160	9	<5	230	82	110	6	1800
02QNM101Lf	5.5	--	0.20	12	0.40	5.2	2.6	0.91	0.24	0.18	0.11	12	640	14	9	230	53	56	500	8	--	22	4	120	37	720	22	67	200	180	180	9	<5	220	74	140	8	2200
02QNM101Lg	6.5	--	0.30	12	0.34	6.2	3.4	1.2	0.27	0.20	0.15	12	250	7	6	160	37	69	240	4	--	27	<4	87	38	750	27	65	110	120	220	10	6	270	94	62	4	1300
02QNM101Lh	7.5	--	0.38	11	0.34	5.8	3.7	1.2	0.26	0.21	0.18	13	560	4	3	120	15	75	130	<2	--	35	<4	74	32	660	25	64	68	52	250	10	<5	320	100	29	2	520
02QNM101Li	8.5	--	0.24	12	0.45	4.9	2.8	1.0	0.27	0.19	0.14	14	800	10	7	190	49	64	380	6	--	25	<4	98	33	970	24	62	150	140	190	10	<5	260	84	100	6	1800
02QNM101Lj	9.5	--	0.18	12	0.55	4.4	1.7	0.73	0.27	0.15	0.07	14	710	16	11	260	80	44	660	10	--	13	6	130	40	1400	22	52	240	240	120	9	8	150	60	180	10	3000
02QNM101Lk	10.5	--	0.23	11	0.54	4.9	2.2	0.90	0.34	0.17	0.11	17	820	12	12	230	92	56	500	8	--	19	4	120	48	1700	23	46	190	250	150	10	5	170	74	130	7	2600
02QNM101Ll	11.5	--	0.21	11	0.56	4.8	2.2	0.93	0.35	0.16	0.11	12	790	11	12	220	93	57	480	7	--	21	4	110	49	2200	22	39	180	240	150	10	<5	160	76	130	7	2600
02QNM101Lm	12.5	--	0.22	10	0.57	4.4	2.0	0.89	0.35	0.16	0.11	13	720	11	11	220	92	55	480	7	--	19	4	110	47	2400	21	39	180	240	140	10	<5	150	71	130	7	2600
02QNM101Ln	13.5	--	0.21	11	0.59	4.7	2.1	0.93	0.33	0.18	0.11	17	780	13	12	240	97	58	550	8	--	20	5	120	48	2600	23	38	200	270	140	10	<5	160	75	140	8	3000
02QNM101Lo	14.5	--	0.22	12	0.63	4.9	2.2	0.97	0.36	0.18	0.12	<10	820	13	13	260	100	60	540	9	1910	21	5	130	51	2700	27	45	210	270	160	10	5	170	79	150	8	2800
02QNM101Lp	15.5	--	0.21	11	0.60	4.3	2.0	0.88	0.33	0.17	0.10	11	740	13	12	260	94	54	530	9	1880	19	5	130	47	2600	27	40	210	260	140	10	5	150	71	160	9	2900
02QNM101Lr	17.5	--	0.22	12	0.57	4.2	2.1	0.84	0.31	0.16	0.11	17	780	14	12	300	77	50	530	11	1820	18	6	150	46	2000	26	51	250	220	140	10	5	180	68	180	10	2700
02QNM101Ls	18.5	--	0.24	11	0.53	4.2	2.4	0.92	0.34	0.16	0.13	16	810	10	11	260	71	55	400	8	2030	24	5	140	46	1900	24	51	200	200	160	10	6	190	75	140	7	2300
02QNM101Lt	19.5	--	0.24	11	0.51	4.1	2.5	0.95	0.31	0.16	0.14	15	810	10	10	260	65	58	390	8	2110	22	5	140	41	2000	26	50	200	190	180	10	6	200	78	140	7	2300
02QNM101Lu	20.5	--	0.23	12	0.58	3.8	2.1	0.88	0.30	0.16	0.11	14	760	13	13	380	100	55	490	10	2180	20	6	190	39	1900	34	58	280	260	150	10	5	160	70	180	10	2800
02QNM101Lv	21.5	--	0.22	12	0.64	3.7	1.9	0.78	0.26	0.15	0.10	17	510	14	14	450	140	47	520	11	2260	18	7	230	36	1800	46	48	340	300	130	9	6	140	62	210	11	2900
02QNM101Lw	22.5	--	0.25	11	0.73	4.7	1.5	0.80	0.24	0.14	0.07	13	280	15	19	500	220	39	570	12	2160	15	8	250	31	2100	96	42	360	450	97	9	<5	110	52	230	12	3900
02QNM101Lx	23.5	--	0.28	12	0.70	4.5	1.5	0.73	0.28	0.16	0.06	11	500	18	20	640	220	44	670	14	2310	13	10	320	38	2200	69	44	450	470	100	10	6	110	53	280	14	4600
02QNM101Ly	24.5	--	0.24	12	0.70	3.2	1.6	0.76	0.36	0.16	0.10	18	670	17	10	600	74	54	650	13	2340	17	9	310	44	2000	68	55	420	200	110	11	<5	130	62	270	13	2800
02QNM101Lz	25.5	--	0.21	14	0.72	2.7	1.4	0.65	0.3	0.14	0.07	16	650	19	11	680	64	46	820	15	2820	14	12	350	36	2000	89	57	490	180	99	10	<5	120	52	320	15	2800
02QNM101Laa	26.5	--	0.24	13	0.65	3.2	1.7	0.72	0.32	0.15	0.10	16	680	17	10	600	76	51	680	13	2840	16	9	310	42	1900	77	60	430	200	110	10	<5	120	58	270	13	2800
02QNM101Lab	27.5	--	0.40	12	0.50	4.4	2.9	1.1	0.34	0.17	0.18	10	320	10	10	350	90	72	420	7	817	29	5	200	51	2000	68	60	230	230	200	12	7	220	89	140	7	2400
02QNM101Lac	28.5	--	0.36	12	0.50	4.0	3.0	1.1	0.49	0.18	0.17	16	1000	8	5	260	51	79	310	5	1880	29	<4	150	51	1800	48	58	160	150	200	12	6	220	96	99	5	1400
02QNM101Lad	29.5	--	0.40	12	0.50	4.0	3.5	1.2	0.40	0.19	0.21	14	1100	6	7	220	38	87	230	4	2150	34	<4	130	42	1700	43	62	130	100	210	12	6	280	110	70	4	1100
02QNM101Lae	30.5	--	0.47	12	0.48	4.5	3.6	1.4	0.40	0.19	0.22	11	860	5	4	170	18	94	140	3	--	32	<4	110	35	1700	40	60	97	68	190	12	<5	320	110	47	2	610
02QNM101Laf	31.5	--	0.31	11	0.57	5.9	2.7	1.2	0.44	0.24	0.17	21	200	8	7	240	77	77	320	5	--	23	<4	150	41	2000	100	47	170	160	130	11	6	200	89	100	5	1500
02QNM101Lag	32.5	--	0.28	9.6	0.66	6.0	1.6	1.1	0.54	0.19	0.16	20	140	8	9	180	94	65	370	5	--	18	<4	100	44	2000	150	39	140	220	100	10	<5	160	77	89	5	1700
02QNM101Lah	33.5	--	0.35	9.9	0.72	6.0	2.6	1.3	0.71	0.14	0.19	13	150	6	6	140	61	78	310	4	--	20	<4	82	48	2000	130	39	100	150	110	12	6	180	91	61	4	1200
02QNM101Lai	34.5	--	0.36	10	0.64	5.6	2.7	1.3	0.63	0.14	0.18	17	140	7	5	130	44	76	280	3	--	21	<4	74	46	1800	130	46	91	110	120	11	6	170	88	52	3	930
02QNM101Laj	35.5	--	0.33	10	0.65	5.7	2.4	1.1	0.54	0.18	0.14	<10	140	8	6	160	58	62	350	4	--	20	<4	88	46	1800	160	45	120	130	130	10	<5	140	75	69	4	1200
02QNM101Lak	36.5	--	0.39	10	0.72	5.6	2.5	1.2	0.57	0.16	0.16	<10	140	9	7	160	58	69	370	4	--	22	<4	88	52	2000	250	42	120	140	140	10	<5	150	77	65	4	1200
02QNM101Lal	37.5	--	0.36	9.8	0.72	5.5	2.6	1.4	0.66	0.13	0.19	<10	130	8	6	120	50	79	340	3	--	20	<4	68	56	2000	360	40	85	120	170	11	<5	170	89	50	3	980
02QNM101Lam	38.5	--	0.38	9.6	0.69	5.6	2.6	1.4	0.67	0.12	0.18	13	130	6	5	110	47	79	290	3	--	18	<4	64	52	1800	300	41	74	120	160	12	7	170	90	42	3	890
02QNM101Lan	39.5	--	0.47	10	0.69	5.6	2.9	1.5	0.77	0.10	0.22	<10	150	5	3	110	25	86	200	2	--	24	<4	65	44	1600	150	42	63	68	160	13	7	190	100	31	2	550
02QNM101Lao	40.5	--	0.44	10	0.71	6.0	2.9	1.4	0.67	0.12	0.20	11	140	6	4	130	39	83	280	2	--	25	<4	77	47	1600	180	46	77	90	180	13	8	200	99	38	3	750
02QNM101Lap	41.5	--	0.53	9.4	0.82	5.4	2.7	1.3	0.66	0.10	0.24	12	180	6	3	230	26	80	160	2	--	28	<4	140	40	1400	88	67	130	64	140	11	6	200	87	60	4	530
02QNM101Laq	42.5	1.56	0.59	9.2	0.90	5.0	2.7	1.2	0.73	0.09	0.27	<10	260	5	3	260	20	81	81	2	--	28	<4	150	37	1200	42	72	140	49	120	11	6	220	85	63	4	400
02QNM101Lar	43.5	--	0.59	8.6	0.90	5.0	2.6	1.1	0.74	0.08	0.26	<10	240	4	2	270	18	72	58	<2	--	27	<4	160	35	1000	49	76	140	42	110	10	5	190	77	65	4	340
02QNM101Las	44.5	--	0.53	8.7	0.92	5.4	2.6	1.0	0.72	0.09	0.25	<10	210	5	3	290	30	66	95	2	--	28	<4	170	36	930	75	80	160	61	96	10	8	170	72	75	4	490
02QNM101Lat	45.5	1.23	0.37	10	0.79	6.5	2.2	1.2	0.53	0.14	0.20	12	150	7	6	170	57	72	270	3	--	21	<4	94	46	1100	180	61	100	120	140	11	5	170	84	55	4	920
02QNM101Lau	46.5	--	0.34	11	0.68	5.4	2.8	1.2	0.45	0.16	0.15	<10	140	8	6	130	56	72	340	4	--	23	<4	72	49	980	180	54	92	140	170	11	6	160	87	51	3	1100
02QNM101Lav	47.5	1.88	0.41	11	0.69	5.0	3.0	1.4	0.57	0.15	0.21	<10	170	8	5	130	43	88	320	4	--	22	<4	76	53	960	140	60	90	120	170	12	7	200	99	48	3	970
02QNM101Law	48.5	2.55	0.45	11	0.69	5.0	3.0	1.5	0.62	0.15	0.23	<10	180	8	4	140	32	95	320	4	--	24	<4	79	54	950	130	59	91	110	160	12	<5	230	100	48	3	870
02QNM101Lax	49.5	2.98	0.43	11	0.68	4.8	2.8	1.4	0.61	0.16	0.21	<10	180	9	4	140	33	89	350	4	--	21	<4	78	54	880	110	55	100	120	140	12	6	220	98	56	4	1000
02QNM101Lay	50.5	2.33	0.45	10	0.65	4.6	2.8	1.3	0.62	0.15	0.22	<10	200	8	4	140	33	85	320	4	--	22	<4	77	52	770	82	59	97	120	140	12	5	210	97	55	4	1000
02QNM101Laz	51.5	2.19	0.47	10	0.69	5.1	2.8	1.4	0.70	0.14	0.24	12	230	8	4	140	37	82	300	4	--	23	<4	76	58	800	62	60	96	110	130	14	<5	190	98	58	4	930
02QNM101Lba	52.5	--	0.55	9.8	0.58	4.6	2.8	1.2	0.64	0.13	0.20	<10	180	7	3	120	36	72	260	4	--	22	<4	72	49	690	49	53	89	110	120	12	6	180	87	51	4	870
02QNM101Lbb	53.5	0.55	0.80	7.8	0.38	2.8	3.0	0.79	0.86	0.07	0.18	<10	580	4	2	80	19	61	110	<2	--	17	<4	50	29	440	27	60	47	56	84	7	<5	160	61	24	2	380
02QNM101Lbc	54.5	0.36	0.78	7.7	0.37	3.0	2.5	0.74	0.89	0.07	0.17	<10	210	4	2	77	17	53	110	<2	--	18	<4	47	25	410	25	58	48	52	77	7	5	170	62	24	2	360

Table A2. Analytical data from the core from Fawn Lake, lower Red River, New Mexico.

[Depth of each subsample, in cm; Cs-137 activity of selected subsamples (dpm/g, dissentigrations per minute per gram); the solid fraction of each sample (dried sample compared to wet sample); and elemental concentrations in weight percent for major elements, parts per million (ppm) dry weight; --, not analyzed. Elemental analyses by ICP-AES following complete mixed-acid digestion (Briggs, 1996); elements analyzed but not detected (Ag, Bi, Th) not reported. Locality coordinates: 36.70633 degrees North latitude; 105.45088 degrees West longitude.]

Field Number	Depth (cm)	Cs-137 Activity (dpm/g)	Solid Fraction	Al %	Ca %	Fe %	K %	Mg %	Na %	P %	Ti %	As ppm	Ba ppm	Be ppm	Cd ppm	Ce ppm	Co ppm	Cr ppm	Cu ppm	Eu ppm	Ga ppm	Ho ppm	La ppm	Li ppm	Mn ppm	Mo ppm	Nb ppm	Nd ppm	Ni ppm	Pb ppm	Sc ppm	Sn ppm	Sr ppm	V ppm	Y ppm	Yb ppm	Zn ppm
02QNM102La	0.5	0.25	0.36	9.4	0.43	5.3	3.3	1.1	0.39	0.19	0.19	11	190	3	4	89	14	65	180	<2	26	<4	58	30	750	21	50	46	48	240	9	<5	210	88	21	2	480
02QNM102Lb	1.5	--	0.44	10	0.40	6.0	3.7	1.2	0.37	0.22	0.22	13	190	3	3	95	6	70	120	<2	27	<4	63	30	560	25	60	46	31	280	10	<5	220	96	15	1	280
02QNM102Lc	2.5	--	0.46	10	0.41	5.7	3.7	1.3	0.41	0.22	0.20	16	190	3	3	95	7	76	120	<2	27	<4	64	30	480	24	54	45	32	320	10	<5	220	99	15	1	280
02QNM102Ld	3.5	--	0.44	10	0.46	5.3	3.4	1.3	0.49	0.21	0.23	14	240	3	4	97	14	79	180	<2	27	<4	64	30	460	24	54	48	45	280	11	<5	220	100	20	2	400
02QNM102Le	4.5	--	0.55	9.8	0.46	5.1	3.3	1.3	0.51	0.21	0.22	<10	290	3	4	93	15	76	210	<2	23	<4	62	30	450	20	53	48	49	270	11	<5	220	98	22	2	460
02QNM102Lf	5.5	--	0.48	10	0.42	5.4	3.5	1.4	0.44	0.22	0.24	<10	260	3	3	95	12	78	190	<2	24	<4	63	30	460	24	59	45	42	310	10	<5	240	100	18	1	380
02QNM102Lg	6.5	0.21	0.45	10	0.41	5.1	3.4	1.3	0.42	0.22	0.24	11	210	3	4	97	10	78	180	<2	25	<4	65	29	450	24	59	47	39	310	10	<5	230	100	17	1	350
02QNM102Lh	7.5	--	0.44	9.1	0.60	5.0	2.9	1.3	0.69	0.16	0.20	10	160	3	4	85	19	82	220	<2	22	<4	55	30	470	27	50	46	51	190	11	<5	200	100	23	2	480
02QNM102Li	8.5	--	0.49	9.6	0.65	5.6	3.0	1.5	0.80	0.19	0.25	10	350	3	4	90	20	95	260	<2	24	<4	58	34	540	24	52	48	57	190	13	5	240	110	25	2	520
02QNM102Lj	9.5	--	0.48	9.8	0.57	5.6	3.1	1.5	0.68	0.22	0.22	15	340	3	3	89	15	99	260	<2	23	<4	59	32	500	26	46	45	51	220	13	<5	250	110	21	2	440
02QNM102Lk	10.5	--	0.39	9.5	0.62	5.7	3.0	1.4	0.63	0.19	0.19	12	180	3	4	86	27	88	280	<2	22	<4	56	31	470	44	43	46	64	210	12	<5	220	110	24	2	540
02QNM102Ll	11.5	--	0.33	8.9	0.70	5.4	2.8	1.2	0.60	0.19	0.21	19	140	3	5	86	36	72	290	<2	20	<4	53	30	470	38	48	49	80	170	11	<5	200	91	31	2	730
02QNM102Lm	12.5	--	0.29	8.5	1.0	5.6	2.6	1.1	0.58	0.18	0.20	11	110	3	6	80	39	66	290	<2	20	<4	50	29	470	34	38	48	89	150	10	6	190	86	32	2	780
02QNM102Ln	13.5	0.46	0.27	7.6	2.9	5.6	2.2	1.1	0.72	0.18	0.17	15	120	3	7	76	67	62	380	2	15	<4	47	30	560	22	34	50	130	110	10	<5	230	78	41	3	1100
02QNM102Lo	14.5	--	0.29	7.6	2.7	5.5	2.1	1.1	0.75	0.19	0.17	11	120	3	8	78	72	64	410	2	17	<4	48	30	600	18	33	52	140	100	11	<5	230	80	45	4	1200
02QNM102Lp	15.5	--	0.36	8.3	2.8	5.0	2.4	1.3	0.88	0.13	0.21	<10	160	3	4	83	39	76	260	<2	20	<4	52	34	620	12	45	49	80	120	12	<5	250	94	32	3	640
02QNM102Lq	16.5	--	0.38	9.0	3.6	5.1	2.7	1.4	0.91	0.13	0.22	13	180	2	3	86	28	84	250	<2	21	<4	54	35	630	15	46	48	67	130	13	<5	280	100	28	2	480
02QNM102Lr	17.5	--	0.35	8.3	5.0	4.8	2.5	1.3	0.70	0.11	0.19	12	150	2	4	82	28	70	230	<2	17	<4	51	31	580	21	39	46	70	150	11	5	270	90	26	2	500
02QNM102Ls	18.5	--	0.40	9.1	2.6	4.5	2.8	1.3	0.71	0.12	0.20	<10	240	3	4	86	31	71	210	<2	22	<4	56	33	610	14	42	48	73	190	11	<5	220	93	28	2	560
02QNM102Lt	19.5	--	0.24	9.3	1.1	4.7	2.8	1.3	0.83	0.13	0.23	<10	250	3	4	93	31	77	210	<2	22	<4	61	34	630	16	50	52	68	190	12	<5	210	100	29	2	500
02QNM102Lu	20.5	0.40	0.43	11	1.4	5.1	3.4	1.5	0.56	0.16	0.22	<10	230	3	4	100	23	87	220	<2	26	<4	70	34	670	18	53	52	66	310	12	5	240	110	24	2	510
02QNM102Lv	21.5	--	0.46	11	1.9	5.0	3.3	1.5	0.56	0.17	0.21	12	320	3	4	99	29	88	260	<2	28	<4	66	34	700	19	50	52	72	270	12	<5	270	110	26	2	600
02QNM102Lw	22.5	--	0.47	9.9	1.9	4.9	3.0	1.4	0.58	0.16	0.20	15	330	3	4	94	30	85	250	<2	21	<4	61	32	660	20	46	49	70	240	12	6	250	100	25	2	570
02QNM102Lx	23.5	--	0.46	9.7	1.4	5.0	3.0	1.4	0.65	0.15	0.22	15	430	3	3	92	23	91	240	<2	26	<4	59	33	610	19	51	48	58	210	12	<5	240	110	24	2	490
02QNM102Ly	24.5	--	0.46	15	1.4	7.8	4.6	2.2	0.99	0.24	0.36	<10	510	4	4	150	29	150	350	2	40	<4	94	50	880	34	73	74	81	320	19	5	360	170	34	3	650
02QNM102Lz	25.5	--	0.49	10	0.80	5.3	3.1	1.5	0.65	0.16	0.24	14	440	3	3	98	17	98	230	<2	26	<4	64	33	590	22	50	50	49	220	13	<5	250	120	22	2	410
02QNM102Laa	26.5	0.48	0.51	10	0.81	5.0	3.1	1.4	0.66	0.15	0.22	13	350	3	3	94	17	88	200	<2	25	<4	60	33	540	22	47	48	49	220	12	<5	230	110	21	2	380
02QNM102Lab	27.5	--	0.54	7.7	0.72	3.7	2.4	1.0	0.51	0.12	0.19	<10	400	2	2	72	16	66	140	<2	18	<4	46	24	420	17	41	38	38	170	9	<5	180	82	16	1	290
02QNM102Lac	28.5	0.47	0.50	9.9	1.3	5.0	3.1	1.3	0.77	0.15	0.25	<10	430	3	3	96	22	86	200	<2	22	<4	61	33	590	25	51	50	54	200	12	<5	250	110	23	2	430
02QNM102Lad	29.5	--	0.47	9.4	1.9	5.2	2.9	1.3	0.74	0.14	0.23	12	180	3	3	94	26	82	210	<2	21	<4	59	31	600	29	44	50	60	180	12	<5	260	100	24	2	480
02QNM102Lae	30.5	0.54	0.49	9.9	1.1	4.9	3.2	1.4	0.62	0.15	0.22	11	230	3	3	98	19	86	180	<2	26	<4	58	32	560	24	58	47	46	220	12	<5	220	110	22	2	370
02QNM102Laf	31.5	--	0.48	9.4	0.96	4.9	3.0	1.3	0.58	0.13	0.17	<10	150	3	3	91	20	82	190	<2	26	<4	54	31	560	28	50	44	50	220	11	<5	200	100	20	2	380
02QNM102Lag	32.5	0.62	0.41	8.4	1.5	5.2	2.6	1.2	0.56	0.12	0.17	13	120	3	3	83	28	73	200	<2	23	<4	48	29	550	39	47	42	61	180	10	<5	190	89	23	2	510
02QNM102Lah	33.5	--	0.43	9.3	1.8	5.9	2.9	1.3	0.54	0.11	0.16	15	130	3	4	94	27	74	220	<2	25	<4	54	33	580	41	52	48	63	200	11	7	200	93	25	2	540
02QNM102Lai	34.5	0.72	0.40	9.2	1.5	5.6	2.8	1.3	0.54	0.10	0.16	13	120	3	4	93	31	75	250	<2	26	<4	54	33	580	44	47	48	74	200	11	<5	190	94	28	2	640
02QNM102Laj	35.5	--	0.42	9.2	1.2	5.8	2.8	1.3	0.68	0.11	0.18	<10	140	3	4	92	34	79	260	<2	23	<4	53	34	600	48	42	49	81	180	12	5	190	97	30	2	670
02QNM102Lak	36.5	1.02	0.37	8.9	1.2	5.4	2.7	1.4	0.80	0.10	0.19	12	140	3	4	93	29	79	260	<2	23	<4	54	34	620	41	47	50	75	180	12	5	200	97	30	3	650
02QNM102Lal	37.5	--	0.41	9.0	1.1	5.1	2.7	1.4	0.75	0.10	0.20	10	150	3	4	94	28	86	250	<2	25	<4	54	34	610	36	50	49	71	180	12	5	200	100	30	2	610
02QNM102Lam	38.5	1.13	0.44	8.8	0.84	4.9	2.7	1.4	0.77	0.10	0.20	<10	170	3	3	94	23	86	260	<2	22	<4	55	34	590	37	45	48	64	160	12	<5	200	100	29	3	570
02QNM102Lan	39.5	--	0.47	8.8	0.82	4.8	2.7	1.3	0.84	0.11	0.22	<10	180	3	3	90	24	84	250	<2	24	<4	52	34	560	33	51	47	60	160	12	<5	200	100	29	2	540
02QNM102Lao	40.5	1.13	0.49	8.6	0.77	4.6	2.6	1.3	0.82	0.11	0.22	11	200	3	3	91	19	85	240	<2	22	<4	53	33	540	28	50	46	56	150	12	<5	200	99	28	2	500
02QNM102Lap	41.5	--	0.49	9.0	0.78	4.7	2.8	1.4	0.79	0.11	0.23	<10	200	3	3	97	20	88	250	<2	25	<4	57	34	550	27	54	49	57	170	12	7	210	100	29	2	520
02QNM102Laq	42.5	1.20	0.54	9.6	0.58	4.8	3.1	1.3	0.63	0.13	0.18	13	240	3	2	96	18	86	190	<2	28	<4	57	32	480	21	51	46	42	210	12	<5	180	110	20	2	330
02QNM102Lar	43.5	--	0.63	10	0.59	4.5	3.4	1.4	0.67	0.12	0.20	<10	770	2	2	94	11	86	120	<2	28	<4	56	35	450	15	60	43	29	230	12	<5	200	110	17	2	190
02QNM102Las	44.5	1.22	0.60	9.8	0.67	5.0	3.2	1.4	0.65	0.13	0.22	10	250	2	2	97	9	88	160	<2	28	<4	58	35	480	17	58	47	29	180	14	<5	220	110	20	2	220
02QNM102Lat	45.5	--	0.63	11	0.46	5.0	3.7	1.2	0.39	0.15	0.23	<10	240	3	<2	100	<1	80	96	<2	31	<4	63	31	410	20	70	48	20	250	12	<5	230	100	15	1	150
02QNM102Lau	46.5	1.10	0.65	9.7	0.45	4.2	3.3	1.2	0.43	0.14	0.20	<10	320	2	<2	97	3	72	77	<2	28	<4	59	29	420	19	63	44	23	230	10	<5	190	95	14	1	140
02QNM102Lav	47.5	1.60	0.57	10	0.68	4.9	3.3	1.3	0.66	0.12	0.24	16	240	3	2	100	15	78	130	<2	26	<4	61	36	500	41	60	50	38	200	12	<5	190	100	22	2	290
02QNM102Law	48.5	2.48	0.55	9.4	0.77	4.8	3.0	1.4	0.80	0.12	0.22	14	230	3	2	96	16	81	140	<2	26	<4	58	37	500	29	53	48	41	160	13	<5	200	100	24	2	300
02QNM102Lax	49.5	1.76	0.64	8.5	0.61	4.1	2.9	1.1	0.83	0.11	0.18	<10	250	3	2	79	13	74	150	<2	21	<4	47	30	410	22	48	40	38	130	11	<5	190	91	20	2	320

Table A3. Analytical data from debris fans, modern and background sediment samples, and selected mill taillings spill samples, lower Red River valley, New Mexico.
[Elemental concentrations expressed in weight percent or parts per million (ppm) dry weight. Analyses by ICP-AES following complete mixed-acid digestion (Briggs, 1996) elements analyzed but not detected (Bi, Eu, Ho) not reported; -- not analyzed. Samples arranged upstream to downstream (E-W).]

Field Number	Description	Latitude DD	Longitude DD	Al %	Ca %	Fe %	K %	Mg %	Na %	P %	Ti %	Ag ppm	As ppm	Ba ppm	Be ppm	Cd ppm	Ce ppm	Co ppm	Cr ppm	Cu ppm	F ppm	Ga ppm	La ppm	Li ppm	Mn ppm	Mo ppm	Nb ppm	Nd ppm	Ni ppm	Pb ppm	Sc ppm	Sn ppm	Sr ppm	Th ppm	V ppm	Y ppm	Yb ppm	Zn ppm
Modern streambed sediment samples																																						
Red River																																						
02QNM-116S	Sample taken downstream from Hottentot Creek	36.70710	-105.43282	5.8	0.25	2.4	2.2	0.44	0.38	0.07	0.22	<2	<10	380	2	3	64	12	32	72	--	19	33	18	610	6	22	26	32	61	6	<5	170	6	60	12	1	250
02QNM-117S	Sample taken upstream from confluence with Goose Crk.	36.67313	-105.37953	7.3	1.9	4.4	2.2	1.0	1.9	0.12	0.45	<2	<10	840	2	3	66	21	82	28	--	17	34	22	1300	3	21	27	39	25	10	<5	450	6	110	18	2	110
02QNM-115S	Sample taken downstream from SW Hanson Creek	36.69787	-105.47443	6.6	0.34	3.3	2.5	0.65	0.67	0.12	0.24	<2	10	620	3	3	84	25	49	89	--	18	42	23	880	14	23	40	57	88	6	<5	210	5	66	20	2	430
02QNM-114S	Sample taken upstream from Columbine Creek	36.68218	-105.51032	6.6	0.32	3.3	2.4	0.66	0.67	0.12	0.26	<2	15	790	3	3	90	26	50	84	--	18	45	22	910	10	26	43	58	76	7	<5	230	5	67	21	2	470
02QNM-112S	Sample taken downstream from Columbine Creek	36.68378	-105.52230	6.8	0.35	3.3	2.5	0.66	0.72	0.12	0.28	<2	14	970	3	4	92	25	50	81	--	19	46	23	1100	10	27	44	60	74	7	<5	240	5	68	21	2	470
02QNM-111S	Sample taken upstream from Goat Hill Campground	36.68737	-105.53987	6.9	0.44	3.0	2.5	0.70	0.88	0.11	0.27	<2	<10	1100	3	4	82	19	51	86	--	19	43	23	840	13	27	40	71	74	7	<5	240	5	69	24	2	540
02QNM-110S	Sample taken at stream gage site	36.70332	-105.56820	7.2	0.36	3.2	2.6	0.66	0.87	0.11	0.24	<2	12	1100	4	4	94	24	54	120	--	20	47	24	1200	11	22	45	69	72	7	<5	240	5	69	25	2	600
02QNM-118S	Sample taken 4 mi downstream from Questa Ranger Station at Red River State Fish Hatchery	36.68420	-105.64925	6.8	0.68	2.7	2.4	0.62	1.5	0.08	0.23	<2	<10	1000	3	3	77	21	44	74	--	17	40	23	870	14	26	37	58	59	7	<5	240	6	63	22	2	520
Tributaries																																						
03QNM201S	Hottentot Creek	36.70780	-105.42975	8.6	0.22	3.4	3.2	0.6	0.3	0.13	0.24	<2	13	1100	2	<2	94	<1	48	20	1540	26	50	22	180	23	32	37	10	150	7	6	170	12	77	13	1	44
03QNM202S	SE Straight Creek scar tributary	36.70882	-105.43720	9.1	0.66	5.8	3.3	1.7	0.9	0.27	0.30	2	16	790	2	2	89	2	99	46	1340	24	53	26	650	21	22	33	17	340	11	<5	280	10	120	8	<1	110
03QNM203S	SE Straight Creek scar tributary	36.70843	-105.44090	8.8	0.21	5.8	3.4	1.2	0.6	0.23	0.22	3	17	960	2	2	93	5	66	52	1680	22	56	29	440	32	24	33	17	330	9	20	230	14	93	11	1	100
03QNM204S	Straight Creek	36.70733	-105.44407	7.4	0.35	4.6	2.9	0.9	0.6	0.17	0.23	2	13	930	2	<2	81	4	58	52	1470	19	48	27	380	32	26	29	15	230	8	<5	180	11	79	12	1	90
03QNM205S	Tributary upstream from Hanson Creek	36.70375	-105.46072	7.1	1.1	4.1	2.7	0.8	1.2	0.16	0.41	<2	14	1100	3	<2	98	12	71	70	1090	19	50	21	500	90	31	42	25	100	9	<5	340	10	88	24	2	130
03QNM206S	Hanson Creek	36.70390	-105.46178	8.6	0.36	4.8	3.2	0.7	0.4	0.15	0.31	<2	18	940	3	2	120	9	68	34	1480	28	64	24	310	12	35	50	24	73	9	<5	250	12	84	25	2	81
03QNM207S	SW Hanson Creek scar tributary	36.70225	-105.46423	8.3	0.65	6.1	3.1	1.3	0.8	0.24	0.30	<2	20	690	2	2	86	6	88	35	1430	23	51	22	420	23	19	34	23	120	10	<5	550	10	110	8	<1	71
03QNM208S	Sediment from catchment basin near Red River across road from Molycorp mill	36.69515	-105.48810	9.8	0.35	5.2	3.4	1.0	0.5	0.21	0.25	<2	17	1100	3	2	100	12	74	92	1580	28	54	27	530	34	27	42	31	170	10	<5	250	12	100	16	2	160
02QNM-113S	Columbine Creek sediment sample	36.67712	-105.51517	7.2	1.6	4.8	2.0	0.94	2.6	0.08	0.35	<2	<10	840	2	3	64	15	66	27	--	14	36	27	750	3	36	27	24	57	11	<5	260	8	97	20	2	150
Composite talus fan samples																																						
03KVTF10	Mallete Creek tributary fan	36.72503	-105.39968	7.0	0.88	2.7	2.8	0.6	1.7	0.11	0.25	<2	<10	830	3	2	120	10	30	50	--	19	72	22	1200	11	25	53	19	70	6	5	270	13	56	28	2	210
03KVTF1	Graveyard Canyon fan	36.71107	-105.42058	7.0	0.57	5.2	2.4	0.6	1.0	0.13	0.29	<2	<10	1000	2	<2	78	20	58	38	--	16	41	17	720	28	20	37	32	44	8	<5	270	8	83	16	1	130
03KVTF2	Hottentot Creek fan	36.70787	-105.42995	9.3	0.07	3.9	3.4	0.7	0.3	0.14	0.25	<2	<10	1100	2	<2	110	<1	54	22	--	28	58	23	180	24	31	42	10	170	8	6	190	13	84	14	1	41
03KVTF3	Straight Creek fan	36.70853	-105.44403	7.6	0.29	5.3	3.0	0.9	0.5	0.18	0.27	3	18	800	2	<2	96	1	60	47	--	23	57	27	330	33	25	32	13	270	8	<5	200	12	81	9	1	74
03KVTF4	Little Hansen Creek fan	36.70227	-105.46378	8.0	1.0	6.4	3.1	1.3	0.8	0.25	0.27	<2	17	660	2	2	86	7	88	34	--	23	52	21	390	22	19	33	20	120	10	<5	630	9	110	7	<1	60
03KVTF5	Small fan immediately downstream from Little Hanson Creek	36.70175	-105.46722	6.9	1.0	3.2	2.6	0.8	1.3	0.11	0.33	<2	<10	950	3	<2	82	15	73	42	--	16	44	22	900	71	20	34	33	71	9	<5	290	9	81	19	2	140
03KVTF5b	Small fan immediately downstream from Little Hanson Creek (duplicate sample)	36.70175	-105.46722	6.9	2.5	3.2	2.6	0.8	1.3	0.13	0.29	<2	13	950	2	2	88	16	66	44	--	16	45	23	1400	19	17	35	35	94	9	<5	350	10	.80	19	2	200
03KVTF6	Sample from fan remnant of Sulfur Gulch	36.69445	-105.49818	7.9	0.87	5.5	3.0	1.4	1.3	0.19	0.31	<2	<10	1000	4	2	98	8	110	150	--	16	57	32	640	460	19	41	37	98	12	<5	420	16	110	17	1	79
03KVTF9	Little Goathill fan	36.68520	-105.52717	7.9	0.92	6.4	2.8	1.0	1.3	0.20	0.26	<2	<10	1200	3	2	110	23	92	150	--	21	63	31	910	25	18	46	36	170	12	6	470	11	110	14	1	140
03KVTF8	Goathill fan	36.68675	-105.53818	6.9	0.19	4.7	3.2	0.5	0.6	0.10	0.24	<2	14	960	2	<2	86	3	39	41	--	22	49	17	250	45	29	31	10	210	6	13	190	14	66	12	2	37
03KVTF7	Capulin fan	36.69855	-105.54973	8.2	0.62	5.8	3.2	0.8	0.9	0.15	0.26	<2	21	920	4	2	170	10	64	110	--	26	100	31	850	19	29	81	25	190	10	<5	220	15	89	33	2	190
Background sediment sites																																						
03QNMB120	Red River upstream from Goose Creek confluence	36.66387	-105.38068	7.0	1.8	3.6	2.0	1.0	1.5	0.14	0.36	<2	12	860	2	<2	74	16	67	44	--	15	42	30	1100	6	22	36	32	21	12	<5	410	9	92	28	3	100
03QNMB124	Red River upstream from Fawn Lake Camp Grounds	36.70642	-105.44632	6.8	0.69	3.9	2.4	0.9	1.0	0.16	0.23	<2	10	940	2	<2	86	14	68	97	--	16	43	26	630	26	20	44	28	110	9	5	230	8	81	19	2	140
03QNMB121	Red River upstream from Columbine Creek confluence	36.68302	-105.51005	7.4	0.89	5.6	2.6	1.1	1.3	0.19	0.29	<2	20	1100	3	2	110	28	110	120	--	17	58	29	1100	140	17	56	50	90	11	6	330	12	100	28	2	170
02QNM-105Ba	Composite sample from river deposit	36.68058	-105.51112	7.6	0.78	4.1	2.7	1.1	1.2	0.14	0.28	<2	12	1000	3	4	87	16	72	100	--	19	46	29	720	19	26	38	35	100	10	<5	300	6	91	18	2	220
02QNM-105Bb	upstream from confluence with			7.0	0.63	3.4	2.6	0.88	1.1	0.10	0.28	<2	<10	1100	2	3	80	13	63	77	--	18	43	24	600	16	27	34	28	84	8	<5	270	8	77	16	2	130
02QNM-105Bc	Columbine Creek			7.1	0.62	3.5	2.5	0.83	1.0	0.10	0.24	<2	<10	1200	2	2	76	13	57	70	--	19	41	23	550	12	25	34	27	90	8	<5	260	6	76	15	1	120
02QNM-105Bd				6.4	0.64	3.9	2.4	0.76	1.1	0.14	0.26	<2	12	790	2	2	72	11	63	52	--	17	39	20	420	14	20	29	22	84	8	<5	260	6	82	11	1	110
02QNM-106Ba	Composite sample from river deposit	36.68155	-105.51768	7.6	0.71	6.7	2.7	1.2	1.2	0.21	0.28	<2	18	970	3	4	110	27	97	160	--	16	59	30	900	85	17	52	40	100	11	7	300	10	100	22	2	150
02QNM-106Bb	downstream from confluence with			7.4	0.66	7.3	2.6	1.2	1.2	0.23	0.29	<2	18	960	4	4	120	35	86	170	--	12	66	28	1000	110	16	60	38	100	11	<5	290	9	100	26	2	140
02QNM-106Bc	Columbine Creek on pipeline access			7.1	0.68	5.6	2.5	1.2	1.3	0.18	0.31	<2	<10	920	3	3	110	23	88	110	--	18	60	26	830	71	20	47	32	95	10	5	310	8	96	20	2	110
02QNM-106Bd	road			6.7	0.70	5.2	2.5	0.93	1.2	0.17	0.26	<2	<10	940	3	3	100	28	73	100	--	15	53	22	860	82	18	44	28	81	9	<5	280	9	90	18	2	87
02QNM-107Ba	Composite sample from river deposit	36.68433	-105.52565	6.6	0.73	7.9	2.3	0.86	1.0	0.15	0.24	<2	10	1300	2	4	90	28	67	70	--	12	42	22	1200	100	10	40	31	79	9	<5	270	4	82	17	2	120
02QNM-107Bb	downstream from confluence with			6.7	0.88	4.9	2.5	0.86	0.98	0.14	0.24	<2	16	1100	2	3	84	20	68	95	--	16	44	23	1300	60	16	41	34	90	8	<5	260	5	79	18	2	140
02QNM-107Bc	Columbine Creek on pipeline			6.7	1.4	5.4	2.6	0.96	1.0	0.17	0.25	<2	13	520	3	3	92	19	73	110	--	17	49	24	1000	84	19	46	37	74	9	<5	300	8	86	19	2	130
02QNM-107Bd	access road			7.4	0.60	2.8	2.7	0.84	1.2	0.09	0.25	<2	<10	1100	2	2	75	9	62	70	--	19	41	24	300	23	26	31	26	75	8	<5	290	6	80	14	1	110
02QNM-107Be				7.5	0.53	3.8	2.6	0.96	1.1	0.12	0.26	<2	<10	1100	2	2	86	14	69	82	--	19	46	27	380	20	28	39	31	100	9	<5	280	7	84	17	2	140
02QNM-107Bf				7.2	0.78	3.6	2.4	0.95	1.5	0.10	0.25	<2	<10	970	2	2	72	9	67	92	--	18	39	25	360	15	24	31	25	76	10	<5	280	6	83	15	2	140
02QNM-107Bg				7.2	0.88	3.7	2.4	0.92	1.7	0.10	0.25	<2	<10	960	2	3	72	13	58	73	--	18	41	28	560	28	27	32	27	67	10	<5	290	6	77	17	2	160
02QNM-104Ba	Composite sample from tributary fan	36.68483	-105.53405	7.8	1.2	3.9	2.3	0.73	2.3	0.06	0.30	<2	<10	940	4	4	120	24	35	65	--	22	65	41	2200	12	25	52	20	85	12	<5	230	10	61	43	4	280
02QNM-104Bb	on south side of Red River			8.0	0.91	3.4	2.9	0.56	2.5	0.05	0.30	<2	<10	790	5	3	94	11	27	35	--	23	45	27	1200	7	35	30	14	120	9	<5	210	16	61	26	3	180
02QNM-104Bc	downstream from Goat Hill Gulch			7.5	0.79	2.8	2.8	0.51	2.6	0.05	0.21	<2	<10	900	4	2	100	6	24	35	--	22	50	26	1000	5	33	38	15	96	8	<5	160	11	42	28	3	180
02QNM-104Bd				7.5	1.1	2.9	2.7	0.59	2.2	0.06	0.24	<2	<10	890	3	3	100	9	35	34	--	21	55	27	1100	4	32	42	17	84	8	<5	170	11	49	31	3	200
02QNM-103Ba	Composit sample from Goat Hill	36.68538	-105.53405	7.9	0.04	4.0	3.4	0.49	0.41	0.12	0.20	<2	14	500	2	2	130	3	41	38	--	28	71	16	220	31	36	48	8	240	7	6	310	10	66	7	<1	47
02QNM-103Bb	Gulch fan			8.0	0.04	4.0	3.6	0.51	0.4	0.10	0.21	<2	<10	670	2	2	110	2	37	34	--	30	61	15	180	19	40	42	7	220	6	<5	240	10	64	8	<1	35
02QNM-103Bc				5.7	0.22	11	2.1	0.59	0.96	0.43	0.18	<2	16	880	3	5	44	17	60	85	--	7	26	16	260	100	11	24	16	58	9	<5	210	7	73	7	1	56
02QNM-103Bd				7.1	0.04	3.8	3.3	0.43	0.38	0.12	0.20	<2	10	520	2	2	97	1	37	37	--	26	53	14	170	22	36	37	6	200	6	<5	160	9	59	8	<1	28
03QNMB123	Upstream from Capulin Canyon	36.69425	-105.54672	7.7	0.69	4.8	2.5	1.1	1.2	0.16	0.25	<2	10	920	3	<2	100	36	82	170	--	20	50	32	1400	64	17	51	36	97	11	5	310	12	95	21	2	150
02QNM-108Ba	Red River alluvial deposit about	36.70082	-105.55785	7.6	0.91	4.8	2.4	1.3	1.5	0.18	0.38	<2	13	1400	3	3	100	19	93	84	--	20	51	30	590	35	23	46	40	77	11	<5	370	8	100	20	2	170
02QNM-108Bb	1 mi upstream from USDA FS			6.2	1.1	10	2.0	0.95	1.1	0.19	0.26	<2	16	900	4	5.	94	42	62	110	--	11	46	23	2500	130	<4	52	46	58	10	<5	290	6	84	24	2	190
02QNM-108Bc	Ranger Station at Eagle Rock Lake			6.8	0.75	3.8	2.5	0.82	1.0	0.11	0.25	<2	<10	1300	3	3	82	17	62	76	--	18	44	24	760	29	24	36	31	83	8	<5	280	7	80	16	2	170
03QNMB122	Red River upstream from USDA Questa Ranger Station	36.70242	-105.56493	7.1	0.56	4.2	2.4	1.0	1.2	0.16	0.27	<2	14	840	3	<2	87	15	81	120	--	20	48	26	690	64	23	44	32	74	10	<5	290	12	89	20	2	110
Mill tailings samples																																						
03QNM209T	Tailings from pipe line break	36.69470	-105.49610	5.5	1.1	6.8	2.9	0.3	1.4	0.08	0.18	2	10	310	5	2	47	22	44	92	--	8	31	19	310	1100	16	20	25	180	6	<5	220	9	41	7	<1	99
03QNM101T	Tailings from 2 ft inside tailings pipe at Columbine Park pipe yard (Molycorp)	36.68347	-105.52455	0.4	0.41	44	0.14	0.1	0.1	0.05	0.07	21	80	640	<1	14	62	820	<1	1200	--	<4	35	4	360	1600	<4	53	630	1600	9	30	640	6	80	6	<1	850
03QNMGHCGT	Goathill Campground tailings (1981)	36.68935	-105.54152	7.2	1.0	4.7	2.6	1.0	1.4	0.16	0.31	<2	<10	1300	3	2	88	18	81	84	--	17	48	26	890	130	20	40	35	89	10	<5	310	11	100	21	2	160
03QNMCAPT	Tailings from Capulin pipe break site	36.69558	-105.54823	7.6	2.4	1.8	4.4	0.5	1.4	0.13	0.15	<2	<10	700	4	2	64	2	31	140	--	19	40	24	860	370	23	22	20	200	5	<5	400	28	53	17	2	210
03QNM210T	Tailings from pipe line break (1979?)	36.70082	-105.55922	7.0	1.0	3.9	2.4	0.9	1.5	0.13	0.30	<2	13	930	3	2	90	14	67	69	--	16	50	28	870	52	23	40	30	71	10	5	280	14	85	23	2	170
03QNM211T	Tailings from pipe line break (1979?)	36.70128	-105.55937	7.7	0.89	4.5	2.7	1.0	1.2	0.15	0.29	<2	<10	1200	3	2	99	22	83	86	--	18	54	29	990	53	23	45	38	80	10	5	330	13	98	22	2	200

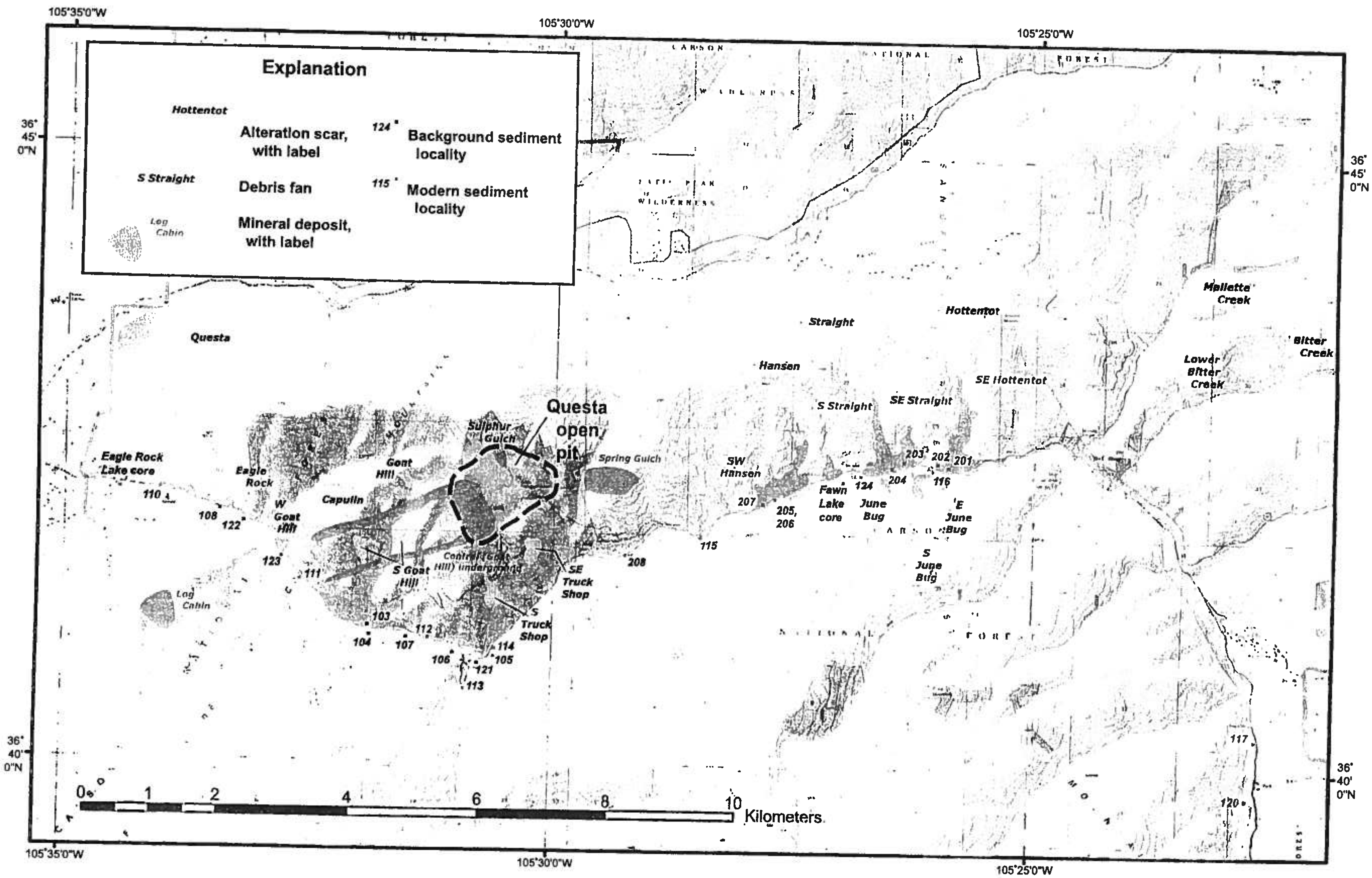
105°35'0"W
105°30'0"W
105°25'0"W
36° 45' 0"N
36° 40' 0"N
Explanation
Hottentot
Alteration scar, with label
S Straight
Debris fan
Log Cabin
Mineral deposit, with label
124
Background sediment locality
115
Modern sediment locality
Questa
Eagle Rock Lake core
110
108
122
Eagle Rock
W Goat Hill
123
111
Capulin
Goat Hill
Log Cabin
S Goat Hill
103
104
107
112
106
121
113
114
105
Sulphur Gulch
Questa open pit
Spring Gulch
SE Truck Shop
S Truck Shop
208
115
SW Hansen
207
205, 206
Hansen
Straight
S Straight
Fawn Lake core
124
June Bug
204
SE Straight
203
202
201
116
E June Bug
S June Bug
Hottentot
SE Hottentot
Mallette Creek
Lower Bitter Creek
Bitter Creek
117
120
0 1 2 4 6 8 10 Kilometers

Fig. 1

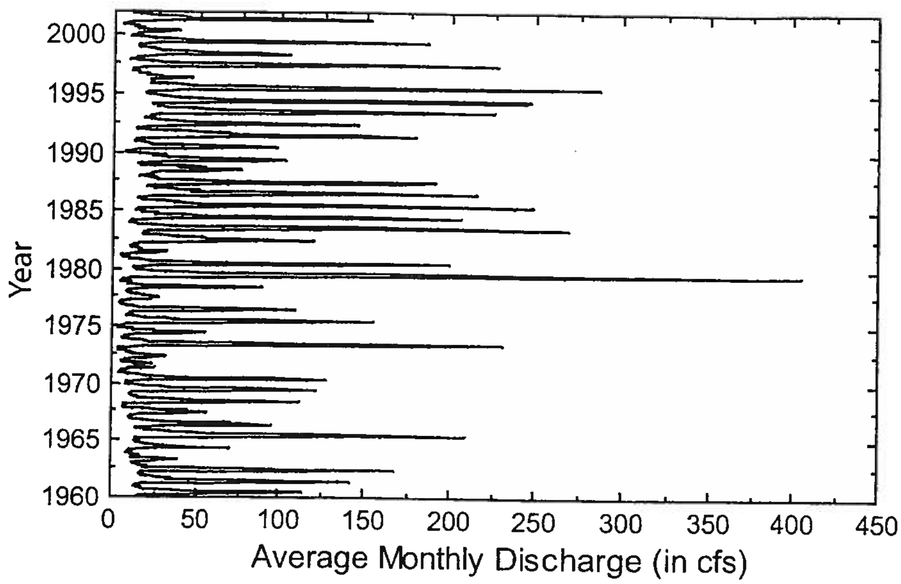

Year
2000
1995
1990
1985
1980
1975
1970
1965
1960
0
50
100
150
200
250
300
350
400
450
Average Monthly Discharge (in cfs)

Fig. 3

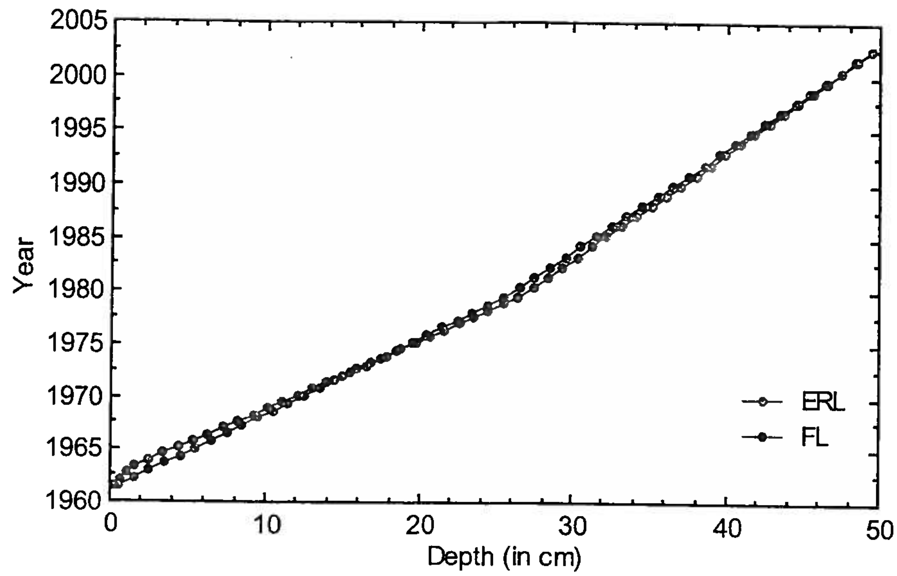
2005
2000
1995
1990
1985
1980
1975
1970
1965
1960
Year
0
10
20
30
40
50
Depth (in cm)
ERL
FL

Fig. 5

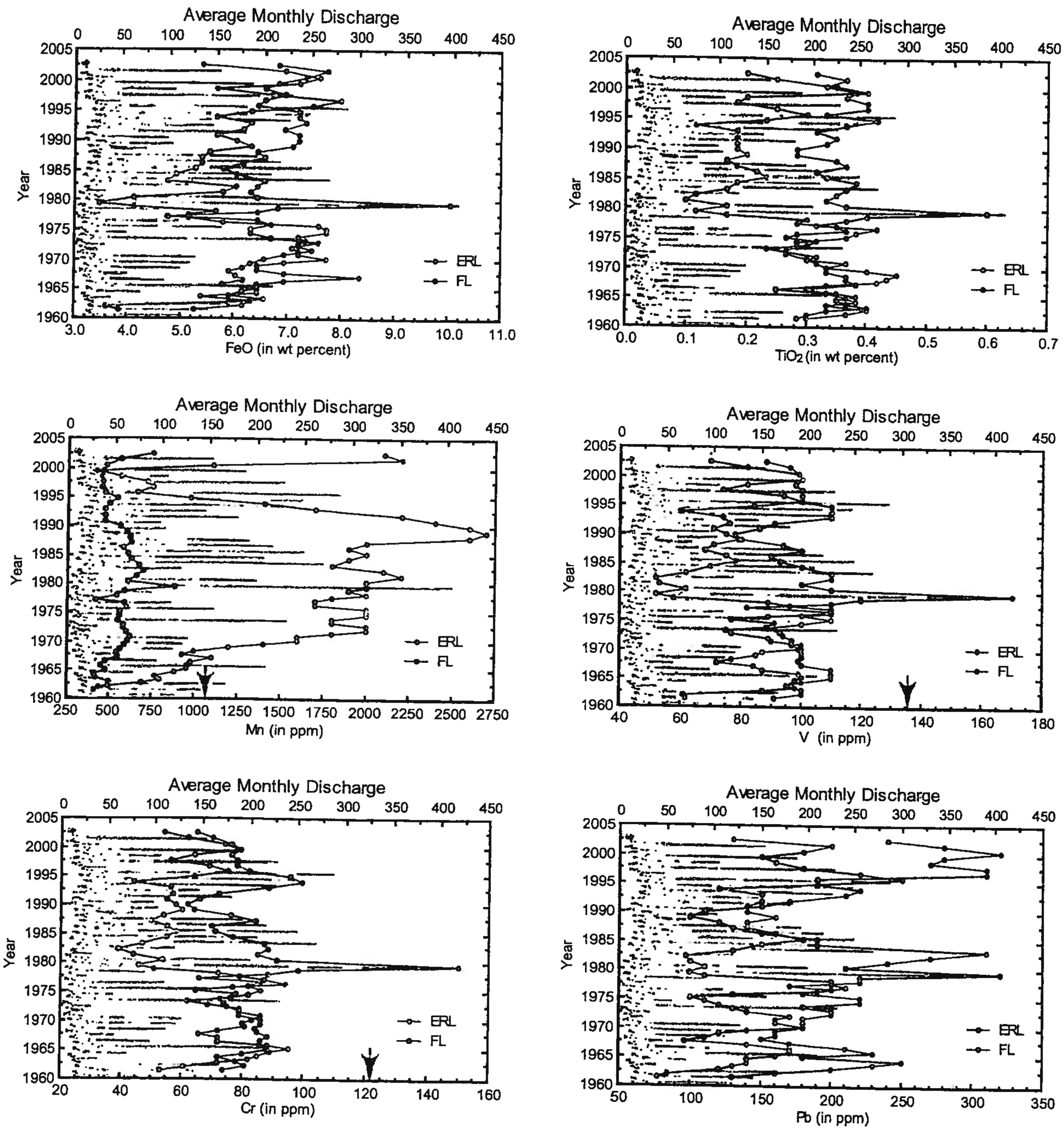
Average Monthly Discharge
Year
FeO (in wt percent)
ERL
FL
TiO2 (in wt percent)
Mn (in ppm)
V (in ppm)
Cr (in ppm)
Pb (in ppm)

Fig7

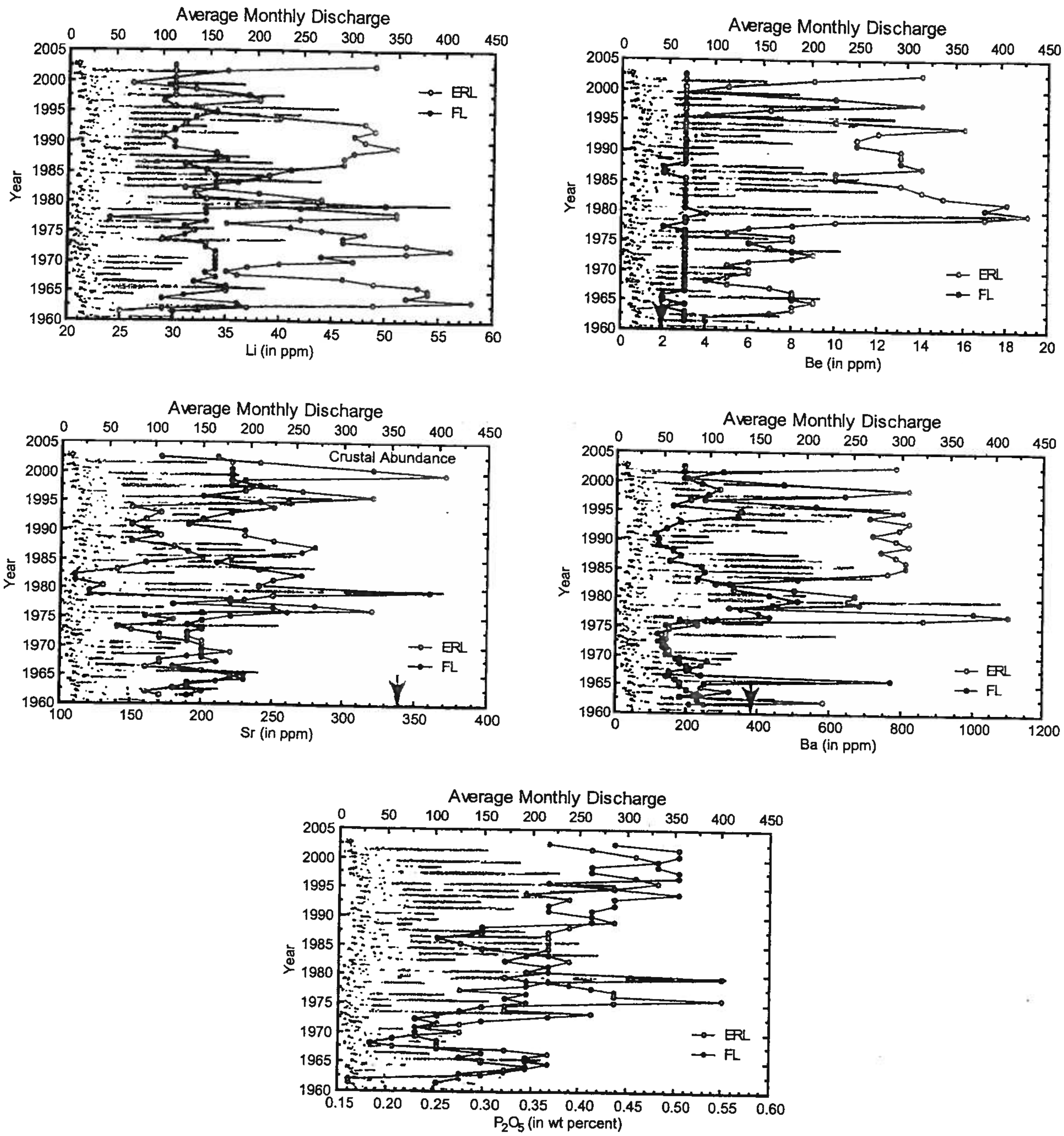
Average Monthly Discharge
Year
Li (in ppm)
ERL
FL
Average Monthly Discharge
Year
Be (in ppm)
ERL
FL
Average Monthly Discharge
Crustal Abundance
Year
Sr (in ppm)
ERL
FL
Average Monthly Discharge
Year
Ba (in ppm)
ERL
FL
Average Monthly Discharge
Year
P_2O_5 (in wt percent)
ERL
FL

Fig 9

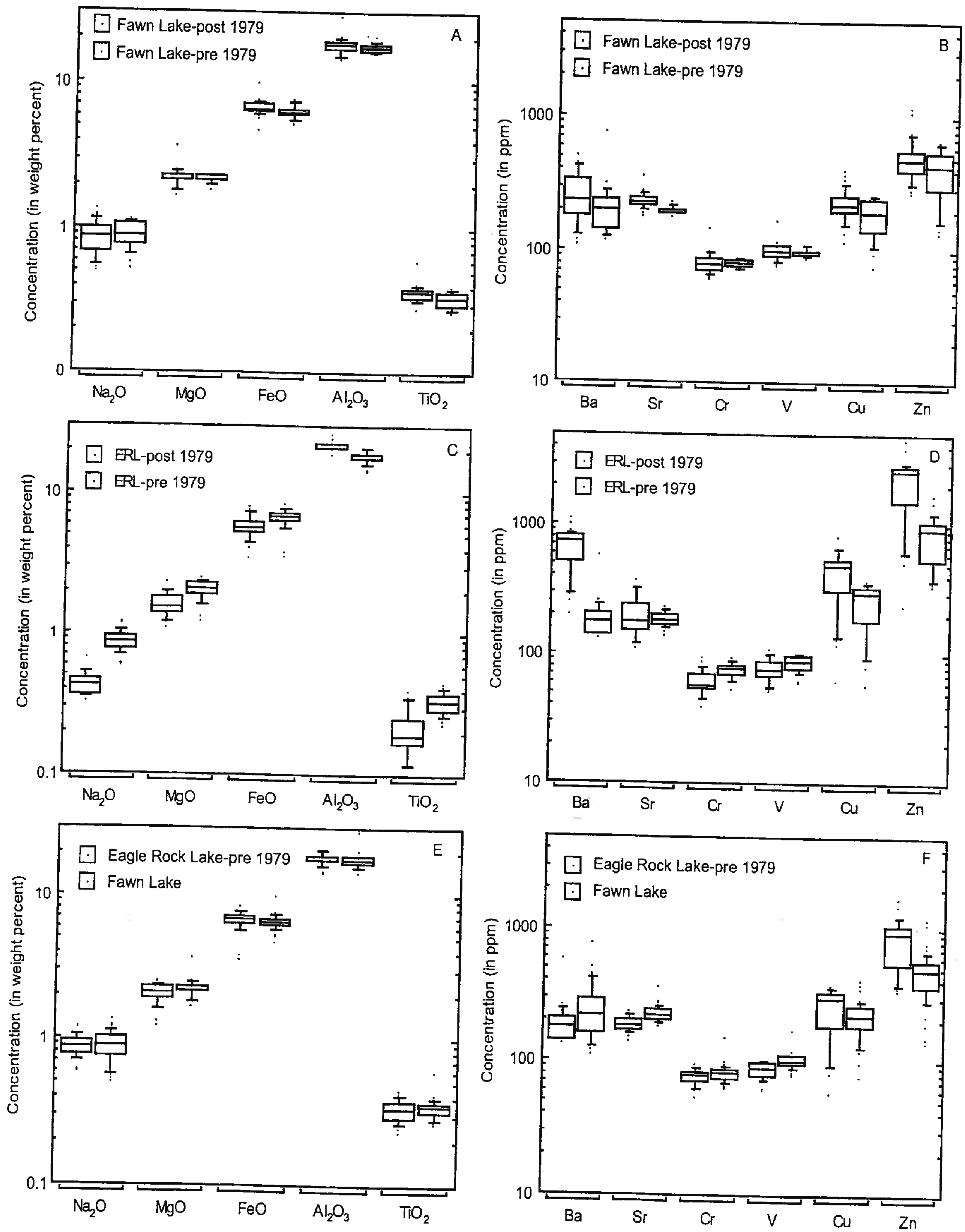

Fawn Lake-post 1979
Fawn Lake-pre 1979
A
Concentration (in weight percent)
Na2O
MgO
FeO
Al2O3
TiO2
B
Concentration (in ppm)
Ba
Sr
Cr
V
Cu
Zn
ERL-post 1979
ERL-pre 1979
C
D
Eagle Rock Lake-pre 1979
Fawn Lake
E
F

Fig 11

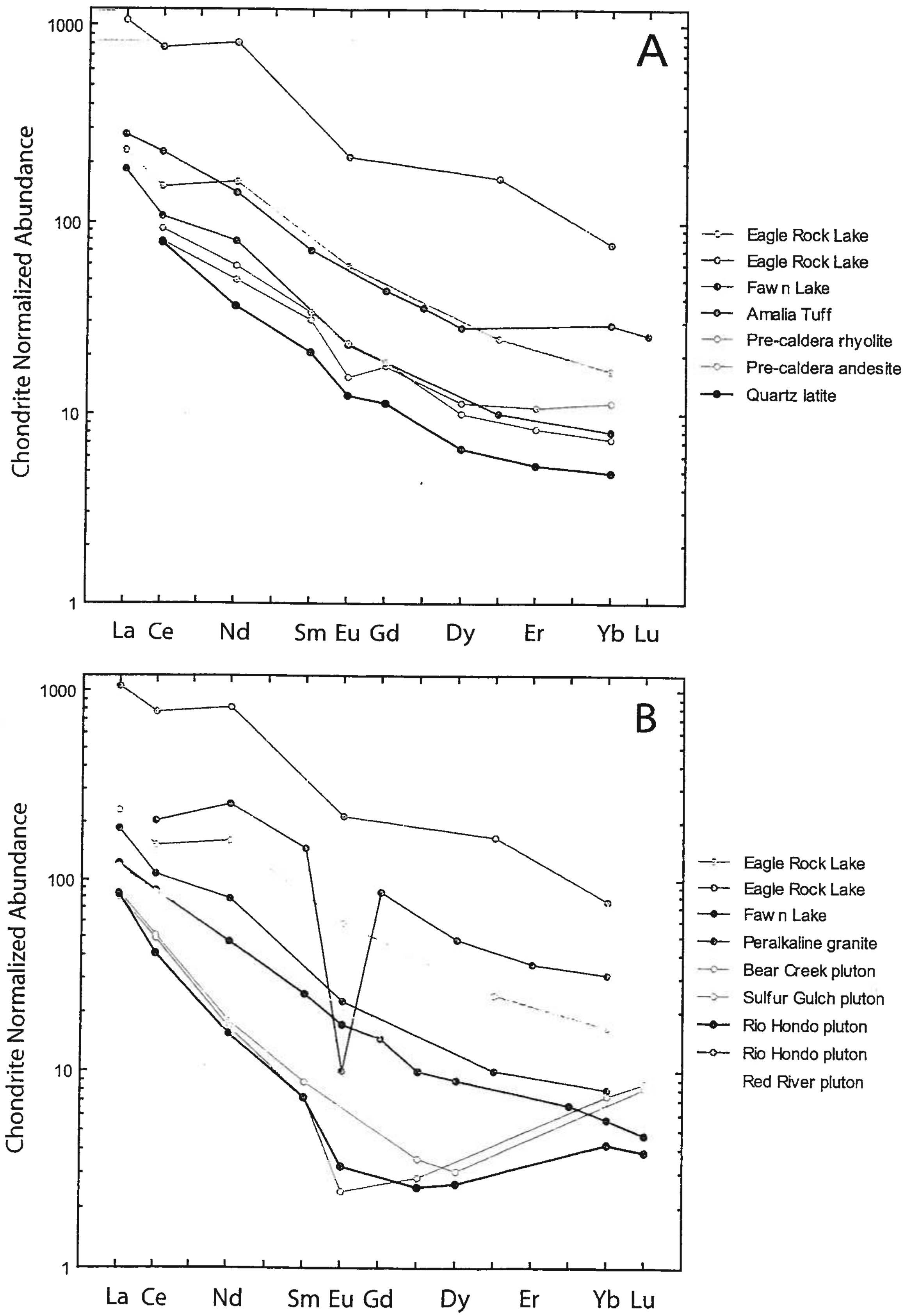
A
Chondrite Normalized Abundance
1000
100
10
1
La Ce Nd Sm Eu Gd Dy Er Yb Lu
Eagle Rock Lake
Eagle Rock Lake
Faw n Lake
Amalia Tuff
Pre-caldera rhyolite
Pre-caldera andesite
Quartz latite
B
Chondrite Normalized Abundance
1000
100
10
1
La Ce Nd Sm Eu Gd Dy Er Yb Lu
Eagle Rock Lake
Eagle Rock Lake
Faw n Lake
Peralkaline granite
Bear Creek pluton
Sulfur Gulch pluton
Rio Hondo pluton
Rio Hondo pluton
Red River pluton

Fig 13

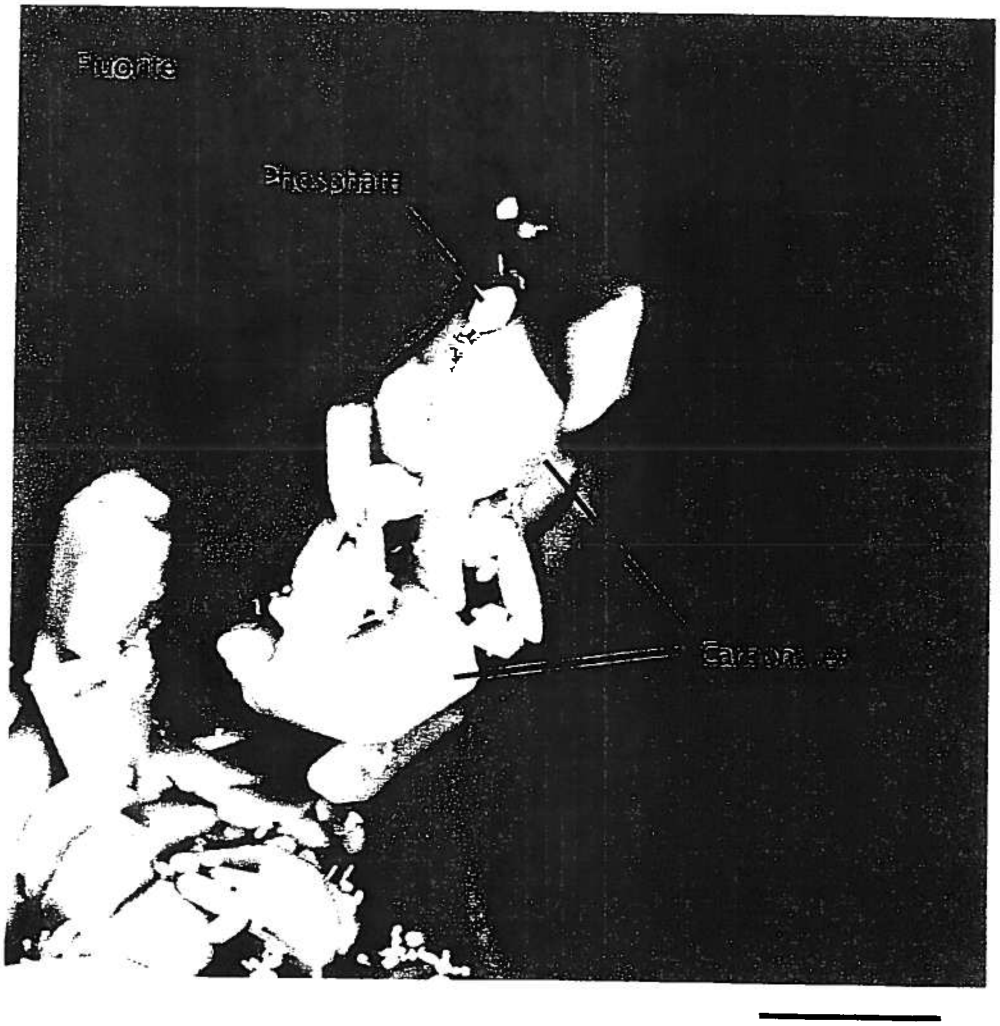

5 microns

Fig. 15

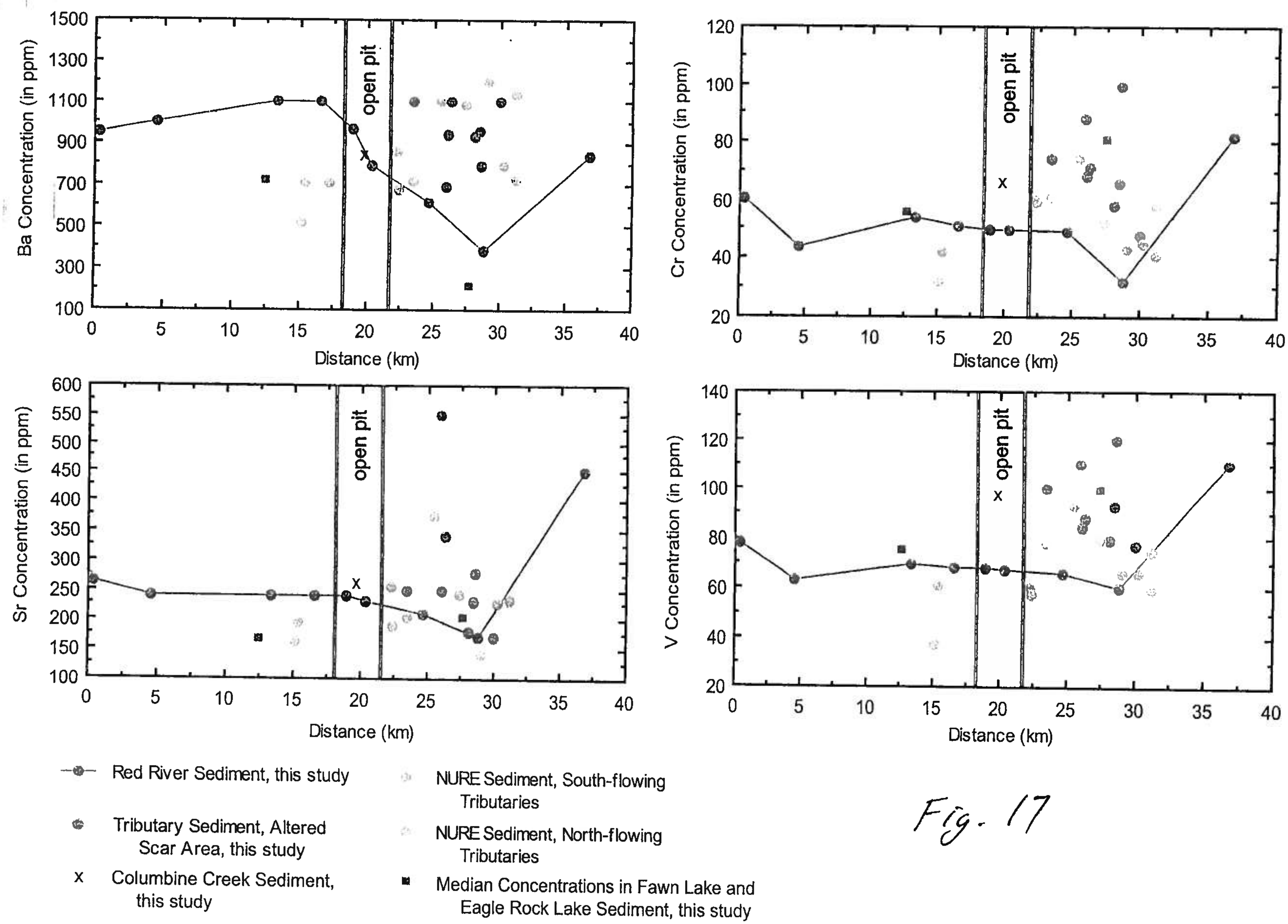

Ba Concentration (in ppm)
Cr Concentration (in ppm)
Sr Concentration (in ppm)
V Concentration (in ppm)
Distance (km)
open pit
Red River Sediment, this study
Tributary Sediment, Altered Scar Area, this study
Columbine Creek Sediment, this study
NURE Sediment, South-flowing Tributaries
NURE Sediment, North-flowing Tributaries
Median Concentrations in Fawn Lake and Eagle Rock Lake Sediment, this study

Fig. 17

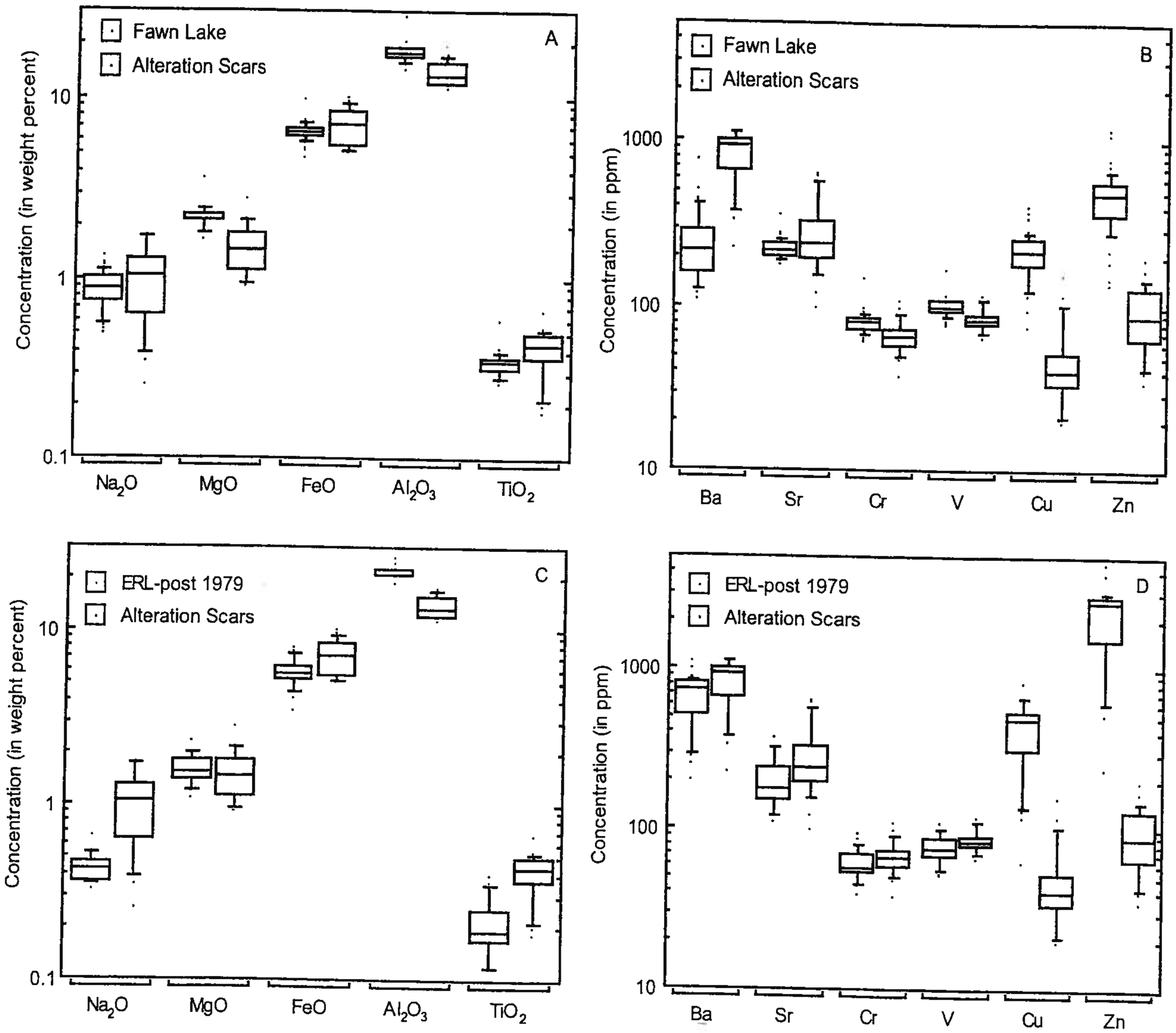
Fawn Lake
Alteration Scars
A
Concentration (in weight percent)
10
1
0.1
Na2O
MgO
FeO
Al2O3
TiO2
Fawn Lake
Alteration Scars
B
Concentration (in ppm)
1000
100
10
Ba
Sr
Cr
V
Cu
Zn
ERL-post 1979
Alteration Scars
C
Concentration (in weight percent)
10
1
0.1
Na2O
MgO
FeO
Al2O3
TiO2
ERL-post 1979
Alteration Scars
D
Concentration (in ppm)
1000
100
10
Ba
Sr
Cr
V
Cu
Zn

Fig. 19

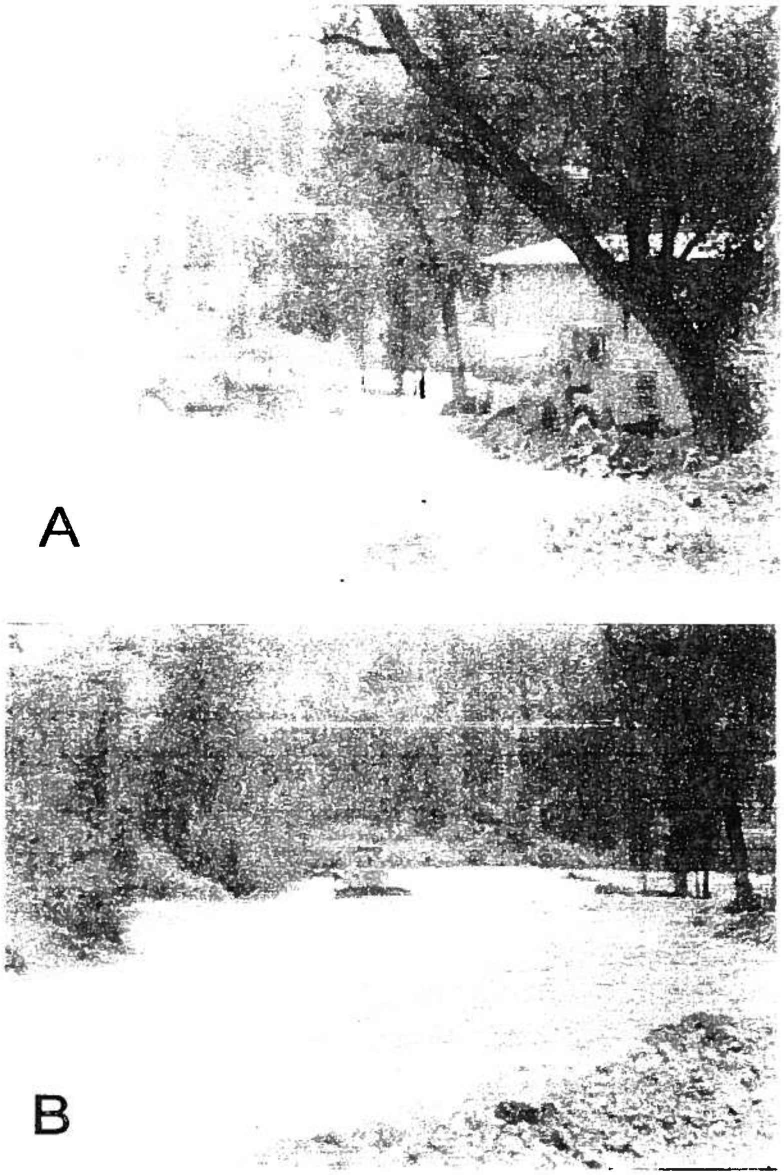

Fig. 21